Investigation of Glutamate Receptors at the Murine Neuromuscular Junction

Stephen Michael Smith
Biomedical Science
The Ohio State University, '09

Honors Thesis
College of Medicine
Submitted May 19, 2009
Defended May 26, 2009

ABSTRACT

Skeletal muscle is composed of two muscle fiber-types: Slow Oxidative (Type 1) and Fast Glycolytic (Type 2). As each muscle's functionality is dependent upon its fiber-type ratio; disruption of muscle fiber-type differentiation directly disrupts muscle physiology. Since fiber-type and overall muscle physiology are partially dependent upon innervation of a muscle fiber by a motor neuron, many muscular dystrophies and atrophies are associated with abnormalities of the neuromuscular junction (NMJ). Here, we characterize novel glutamate receptors at the NMJ, focusing primarily on the obligate N-methyl-D-aspartate (NMDA) receptor subunit, NR1. First, we determine the timing of localization to the junction and begin to identify which NR1 isoforms are expressed in muscle. Then, we analyze electrophysiology experiments to detect changes in skeletal muscle membrane potential after treatment with glutamate receptor agonists/antagonists. Finally, we use *Cre-loxP* technology to create muscle-specific knockout mice for NR1. From these studies, we determine that NR1 localizes to the NMJ between 1 day and 1 week of age in mice. We further conclude that glutamate receptors at the NMJ are functional, based upon changes in quantal content and mini end-plate potential (mEPP) frequency after antagonist treatment. Our preliminary data suggests the presence of at least two alternatively spliced NR1 isoforms in muscle; however we were unable to definitively identify the sequences of these isoforms. Overall, these results challenge the conventional dogma of a "simple synapse" mechanism of neuromuscular transmission, providing the possibility of alternative methods of treatment and therapeutics for muscular dystrophies and other neuromuscular disorders.

ACKNOWLEDGEMENTS

Certainly, this journey could not be possible without the Principal Investigator, Dr. Jill Rafael-Fortney. I am indebted for her dedication in training me, ability to reason and work with me, trust and faith in me. To my advisors, Dr. Bruce Biagi and Lori Martensen—who have listened to my grandiloquent and often puerile complaints—I can't imagine completing this project without your support and guidance; I sincerely appreciate your attentive counsel and confidence.

Thank you, Jamie Sanford and Dawn Delfín, for your guidance, affable nature and for reviewing this thesis. A special thanks to Tess, Alina, Niya and Steve for a palatial friendship abundant in laughter and blithesome discourse. Much appreciation to Dr. Luis Polo-Parada for his expertise in physiology and for agreeing to complete the physiology experiments; Dr. Margaret Teaford for serving as a representative to my thesis committee and helping me to navigate the honors program; and to Dr. Paul Jansen for his consultation on the statistical analyses. Many thanks to the University Research Office (Helene, Allison and Suzanne) for their continued advice and support, and for enabling me to serve as a URO Fellow for 2008. To ULAR, for their unceasing dedication of watching the mice scratch themselves.

"Thank you." It is a simple trip of the tongue, yet two syllables that I neglect all too often. So many are due this sentiment, and yet, despite the recognition inscribed herein, I suspect there are a great many I will have absent-mindedly forgotten. And for that, I do apologize, but I thank you nevertheless, for you too have made a difference.

TABLE OF CONTENTS

I

Introduction

Significance

Duchenne muscular dystrophy (DMD) is a recessive X-linked disorder which affects 1 in 3000 male births. Affected individuals experience severe skeletal muscle weakness and eventually a complete loss of muscle control until succumbing to respiratory or cardiac failure. Prognosis is variable, but average survival range is between 14.4 and 20.5 years of age [**15**]. Modern treatment options such as antibiotics and assisted ventilation have greatly improved life expectancy [**16**], but have not significantly increased the median survival age [**30**].

The DMD gene has been cloned and encodes for *dystrophin* [**11, 17, 19, 26, 75**], a 427 kDa structural protein which functions to (1) connect the basal lamina surrounding the sarcoplasmic skeletal muscle membrane to the cytoskeleton under the sarcolemma [**36, 43**], and (2) interact with major functional membrane proteins which control the flexibility of the sarcolemma during physiological processes [**7, 43, 56**]. Absence or dysfunction of *dystrophin* thereby creates dysfunction in the myocyte's ability to maintain normal structure and function, eventually leading to muscle fiber necrosis.

Arguably, maintenance in skeletal muscle structure would improve both outcome and quality of life for these patients. Although *dystrophin*-replacement therapeutic strategies continue to be researched, developments in the understanding of the pathogenesis of DMD with the ultimate goal of designing treatment strategies have focused on understanding all pathogenic aspects of skeletal muscle, including investigation of the neuromuscular junction.

Skeletal Muscle Physiology: A Brief Review

Skeletal muscle is comprised of elongated, multinucleated fibers (composed of several major proteins including actin, myosin, tropomyosin & troponins) which allow for elasticity and movement. These fibers are classified into two major types: "slow twitch" and "fast twitch." "Slow twitch" (type 1) fibers contain high levels of mitochondria and therefore have a high oxidative capacity. These fibers work primarily by aerobic respiration to produce a lasting duration of action (endurance). "Fast twitch" (type 2) fibers contain fewer mitochondria and thereby require anaerobic respiration (glycolytic), but convey more energy over a shorter duration. The ratio of fiber-types within a given muscle is directly correlated with its overall function. For example, the soleus is a major lower-limb muscle used in plantar flexion (running, walking, etc.) and is comprised primarily of type 1 fibers given its function. In contrast, the extensor-digitorum longus (EDL) of the lower-limb is involved in movement of the distal tarsals, used far less frequently than the soleus. It is predominantly comprised of type 2 fibers.

Important to athletes and post-surgical recovery, the predominant fiber-type of a muscle can be trained. For example, the gastrocnemii of marathon runners would most likely have a higher ratio of type 1 to type 2 fibers, as these runners have trained for increased endurance. Conversely, the same muscle measured in sprinters would probably yield a higher ratio of type 2 to type 1 fibers, as these runners have trained for shorter, "bursts" of energy.

Fiber-type composition and post-synaptic membrane structure have been implicated in DMD. In a severe muscular dystrophy mouse model, Rafael *et. al.* showed that fiber-type ratios were altered to be predominantly oxidative, with an increase in type

1 fibers [**54**]. Webster *et. al.* demonstrated that fast-twitch (type 2) fibers are preferentially affected in DMD, suggesting that the DMD gene product specifically functions in type 2 fibers [**73**]. In many instances of myopathies and dystrophies, fiber-type conversion results in loss of function in key muscles. Thus, understanding the factors leading to fiber-type differentiation is critical to understanding underlying mechanisms of neuromuscular disease. Fiber-type is, in part, determined by the direct innervation of each fiber: larger motor units provide a greater frequency of impulses and larger amounts of energy [**12**]. However, the molecular pathways from innervation leading to fiber-type have not been well characterized [**49**].

The site where a skeletal muscle fiber is innervated by a motor neuron axon is a synapse known as the neuromuscular junction (NMJ). Release of the major excitatory neurotransmitter acetylcholine (ACh) at the NMJ allows for a multistep process called excitation-contraction coupling, which is responsible for muscle contraction [**6**]. After release from the axon, ACh binds to homogenous receptors (AChRs) in the heavily invaginated post-synaptic membrane. Along this membrane are characteristic folds divided by secondary clefts, both of which contain major structural proteins and peptides of physiological significance (*See Figure 1-1*) [**21**]. Disruption of this membrane has been observed in DMD patients [**60**], although the distribution of AChRs has been found as comparable to normal individuals [**70**]. Knocking out *dystrophin* and *utrophin* (a *dystrophin* homologue which partially compensates in its absence) revealed abnormal NMJ topology in mice [**54**].

The NMJ has classically been viewed as a simple “cholinergic synapse”. Recent discovery of glutamate receptors at the mammalian NMJ suggests the possibility of

alternative pathways in which the NMJ might function, or neuromuscular diseases might progress [**38**]. Based on work in vitro, Lee *et al* suggested that glutamate might be released by motorneurons in mammalian skeletal muscle and therefore might be responsible for skeletal muscle differentiation mechanisms [**35**]. At this point, it had not been investigated as to whether glutamate levels or localization vary in an *in vivo* model of skeletal muscle. If glutamate does function at the NMJ, it would follow that glutamate receptors there may be involved. It is intriguing to speculate that the role of these receptors might be involved in determining fiber type or skeletal muscle functionality, but these experiments have not yet been conducted. Identifying the functionality of these receptors is requisite to completely understanding the mammalian NMJ.

Figure 1-1

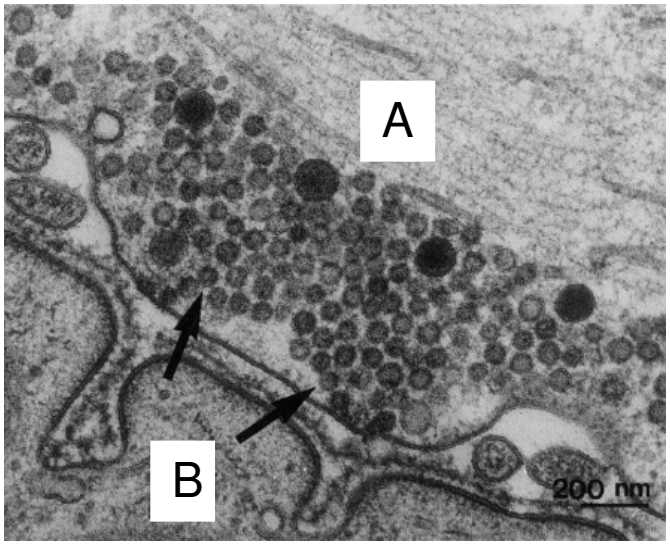

Figure 1-1: Electron micrograph of the NMJ. (**A**) Axon terminal. (**B**) Muscle. Arrows point to pre-synaptic vesicles, containing neurotransmitters. *EM Mimcrograph used with permission of W. Stark, St. Louis University, MO.*

Glutamate Receptors and Cell Signaling

There are three major types of ionotropic glutamate receptors: N-methyl-D-aspartate (NMDA), α-amino-3-hydroxy-5-methylisoxazole-4-propionic acid (AMPA) and kainate receptors (*Figure 1-2*). Ionotropic glutamate receptors, when activated,

become permeable to specific ions (e.g. Ca^{2+}, Na^{+}, K^{+}) dependent upon the composition of the receptor [**13**]. The focus of this thesis is on characterization of the physiological functions of NMDA and AMPA receptors at the murine NMJ, with particular emphasis on NMDA receptors.

Figure 1-2

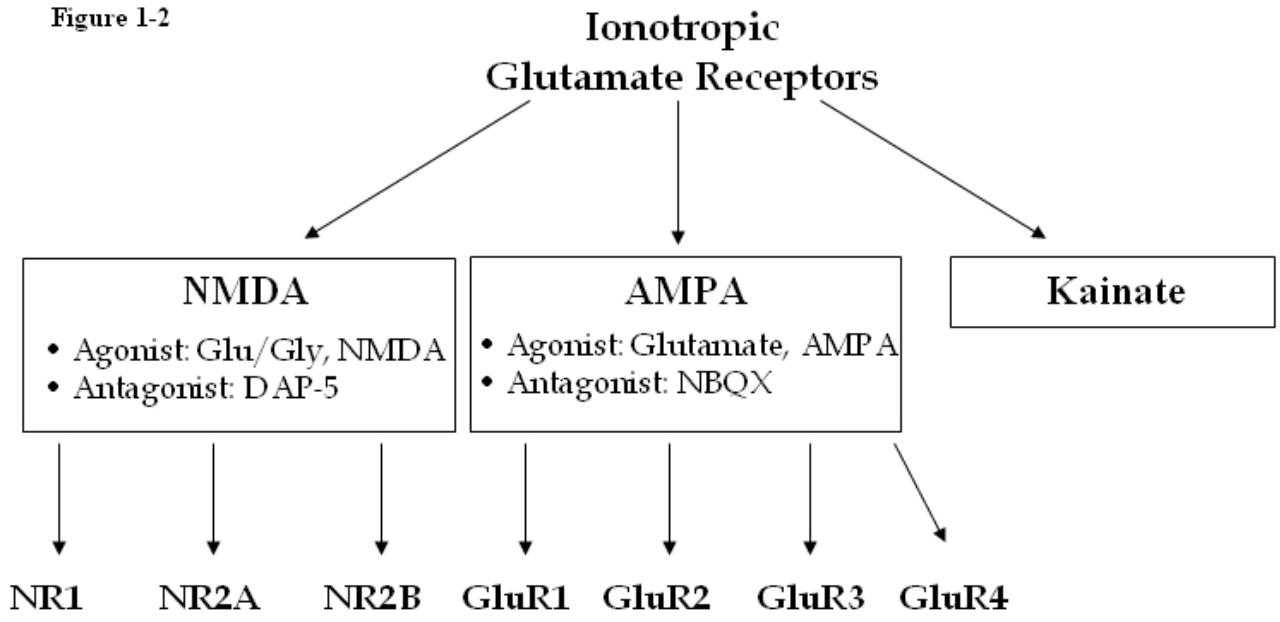

Figure 1-2: Types of glutamate receptors. NMDA receptors include three major structural units, NR1, NR2A and NR2B. AMPA receptors include GluR1-4. This thesis will not focus on kainate receptors.

NMDA receptors are composed of several components, including NMDA receptor subunit 1 (NR1), subunit 2B (NR2B) and subunit 2A (NR2A). NR1 is the obligate functional subunit of NMDA receptors [**67**], containing a high-affinity glycine-binding site which activates the ligand ion channel [**22**]. Alternative splicing of the gene product for NR1 can lead to at least eight different protein isoforms in the brain, each with different localizations and functions (*see Chapter* II). NR1 complexes with NR2x subunits which serve to reduce the potency of glutamate thereby reducing the risk of neuronal glutamate toxicity [**1, 34**]. In the hippocampal region of the brain, glutamate

receptors (particularly NMDA receptors) are linked to memory and learning mechanisms including long-term potentiation [**28, 49**]. If the NR1 subunit is completely knocked-out, mice die within ten hours of birth from respiratory failure or cleft palate [**18**]. Single *et al* showed that dysfunctional NR1 causes death within 1 hour of birth [**66**]. Incidentally, knockout of the NR2A subunit caused no developmental changes in mice [**61**], firmly establishing NR1 as the requisite subunit *in vivo*.

NR1 localizes to the secondary folds of the NMJ, however its function here remains unknown. A single experiment measuring the contraction of rat diaphragms after electrical stimulation and treatment with ACh inhibitors has led to the hypothesis that NMDA receptors may function as a co-transmitter with ACh at the NMJ [**32, 49**]. However, little evidence supports this hypothesis and the functional role of glutamate receptors at the NMJ has not been definitively elucidated.

AMPA receptors are widely expressed throughout the brain and are responsible for the most rapid excitatory neurotransmission in the brain [**10, 50**]. There are currently four subunits known: GluR1, GluR2, GluR3 and GluR4. Unlike NMDA receptors, AMPA receptors do not have an obligatory subunit for functionality [**37**]. AMPA receptors may function individually, or may combine to form heteromeric functional receptors [**27, 62, 72**]. Like NMDA receptors, they have been linked to cell polarity balance [**42**], long-term potentiation [**57**], and calcium permeability [**25, 72**]. Mouse knockouts of GluR1 were "smaller than their litter-mates during the first postnatal weeks, but after weaning, their size was normal" [**77**]. Interestingly, a knockout of GluR2 leads to a phenotype similar to that found in murine model of DMD, including a hunched back, slow movement, and death between 7 and 20 days after birth [**20**]. Though the structure

and physiological function of these receptors have been shown in brain, it has yet to be determined what their structures and functions might be in skeletal muscle.

Objectives

The present studies will test the overarching hypothesis that NR1, the functional and essential subunit of NMDA receptors, functions in the development and maintenance of muscle fibers. Specifically, the goals of this study are to determine: (1) the timing of NR1 localization post-natally; (2) the normal function of glutamate receptors in murine skeletal muscle; (3) the composition of NR1 transcripts in skeletal muscle; and (4) determining the physiological or morphological consequences of ablating NR1 in murine skeletal muscle tissue. These studies are crucial to understanding the complete physiology of the NMJ, having the potential to challenge the dogma prevalent in neuromuscular physiology.

II

Characterization of Glutamate Receptor Subunits at the Neuromuscular Junction

Introduction

Until recently, the NMJ had traditionally been described as a simple cholinergic synapse. In 2009, Mays *et al.* demonstrated post-synaptic localization of AMPA GluR1 and GluR2/3 subunits, as well as NMDA NR1, NR2A and NR2B subunits to the murine NMJ at 5 weeks of age [**38**]. If glutamate receptors contribute to the development of muscle fibers, it would follow that localization of these receptors would correlate with fiber type development and differentiation. We hypothesize that NR1 will localize to the NMJ at a time period prior to or concurrent with fiber type differentiation.

We further investigate the primary structure of glutamate receptor subunits found in skeletal muscle. In the brain, the NR1 protein can be defined by any of eight known splice variants which are regulated developmentally in a cell-specific manner and function in learning and memory [**33, 44, 46, 78**]. These variants arise from alternative splicing of the NR1 gene, which is known to contain 22 exons with splice sites between exons 5, 21 and 22 (*see Figure 2-1*) [**24, 78**]. Alternative splicing incorporates three distinct sequences into the NR1 gene referred to as the α, β, and γ exons. The α exon is the 63 bp sequence known as the "N1 cassette" and can be inserted into the N-terminal domain of the gene. The β (111 bp) and γ (114 bp) exons are adjacent at the C-terminal domain and respectively termed C1 and C2 cassettes, as they determine the primary structure of the NR1 C-terminus. The C2 cassette codes for a "stop" codon, however if the C2 cassette spliced out, then an alternative (C2') cassette coding for a stop codon is

found 66 bp downstream of the "pan region." The "pan region" refers to the translated domain between exon 5 and exon 21, which is common between all known isoforms in the brain [**3, 33, 46, 78**]. Campusano *et al.* have recently described an additional alternative splicing site of exon 11 (located in the "pan region") in embryonic rats, however this isoform has not been detected post-natally [**8**]. *Table 2-1* characterizes the known transcript variants.

NMDA receptor functionality is dependent upon both the type of NR1 isoform present as well as any additional heterodimeric binding that occurs with other NR2x subunits [**76**]. The presence of the N1 cassette significantly decreases agonist affinity and produces faster deactivation (closing of the ion channel) [**14**], whereas its absence increases the effect of L-glutamate (increased permeability of ions through NMDA-receptor ligand channels) [**59**]. In NR1-deficient mouse neurons, Bradley *et al.* showed that reintroducing an NR1 mutant with a deleted C1 cassette greatly reduces the efficiency of NMDA receptor–driven gene expression, without disrupting the Ca^{2+} balance [**5**]. Expression levels of different NR1 isoforms in various brain regions have also been shown to change over the course of development. In the cortex of developing rats, Prybylowski *et al.* showed that C2-containing isoforms initially localizes at 1 day after birth, but then is replaced by C2'-containing isoforms by 7 weeks after birth [**53**]. It therefore is likely that while one isoform is predominant in skeletal muscle at a certain time post-natally, it might be replaced as necessary function for the receptor is altered.

Table 2-1

Name of Splice Variant	Alternative Exon Presence			Total Size of NR1 (bp) gene product
	α	β	γ	
$NR1_{000}$	-	-	-	2655
$NR1_{001}$	-	-	+	2703
$NR1_{010}$	-	+	-	2766
$NR1_{011}$	-	+	+	2814
$NR1_{100}$	+	-	-	2718
$NR1_{101}$	+	-	+	2766
$NR1_{110}$	+	+	-	2829
$NR1_{111}$	+	+	+	2877

Table 2-1. NR1 gene splice variant description. Subscripts: "0" corresponds with "-", meaning the alternative exon is not included in the transcription; "1" corresponds with "+", indicating the exon is included in the transcription for α, β, γ, respectively. The α exon corresponds with the N1 cassette (66 bp); the β exon is the C1 cassette (111 bp); the γ exon refers to a C-terminus cassette C2 (114 bp), which splices in to prevent translation of the terminal sequence C2' (66 bp).
Table adapted from Zukin *et al.* [**78**]

As NR1 and other glutamate receptors were recently discovered at the NMJ, it is not known whether these receptors are of the same amino acid sequence as those expressed in brain, or if other exons are alternatively spliced to create novel protein isoforms. Based upon known splicing of NR1 in the brain and data gathered from the localization experiments, we hypothesized that there are multiple splice variants of NR1 expressed at the skeletal muscle NMJ.

We therefore designed experiments to determine when NR1 and other glutamate receptor subunits localized to the NMJ after birth; to determine if NR1 localizing to the NMJ correlated chronologically with fiber type development and differentiation; and to determine if the receptor subunit protein isoform(s) expressed in muscle was similar or identical to those expressed in brain. We utilized immunofluorescence to determine NR1 localization in skeletal muscle, immunoblotting for confirmation, and fiber-type analysis to determine chronologic correlation. We then used PCR amplification of reverse-

transcriptase (RT-PCR) of skeletal muscle mRNA with primers designed against several glutamate receptor subunits, allowing for expressed DNA (cDNA) to be sequenced for comparison against expressed receptor proteins in brain.

Methods

Immunofluorescence

8 µm sections of unfixed frozen quadriceps from C57 Bl/10 mice aged 1 day, 1 week and 1 year, were blocked with 1% gelatin in potassium buffered saline (KPBS) for 15 min at room temperature and rinsed for 5 min in KPBS. Sections were then incubated for 2 hours with polyclonal rabbit anti-NR1 antibody (Chemicon, 1:50 dilution) diluted in KPBS with 0.2% gelatin (KPBSG) and 1% normal goat serum. Slides were then rinsed 3 x 5 min in KPBSG. After rinsing in KPBSG, the secondary antibody, CY3 α-rabbit 1:200 dilution) in a mixture of KPBSG and Alexa 488-conjugated α-bungarotoxin (1:1000) with 1% normal goat serum was applied and incubated for 1 hour at room temperature. α-bungarotoxin binds to endogenous nicotinic AChRs and thereby labels the NMJ. Slides were mounted and coverslipped with Vectashield® and the DNA-binding dye, DAPI. Tissues incubated with only secondary antibody was utilized as a negative-control. Images were taken through a Nikon Eclipse 800 epifluorescence microscope using a SPOT-RT slider digital camera and Spot® software.

Immunoblots

Total skeletal muscle from 10-week-old C57 Bl/10 mice were homogenized in Newcastle buffer (4 M Urea, 75 mM Tris, pH 6.8, 3.8% SDS). Protein concentration was determined using the Biorad DC protein quantization kit by measure absorbance of samples on a spectrophotometer (Beckman Du-64) at 750 nm. 100 µg protein was then run out on 8% SDS-polyacrylamide gel electrophoresis (SDS-PAGE) gels at 80 V.

Proteins were then transferred from SDS-PAGE gels to nitrocellulose (Whatman International) at 80 V for 45, 80 or 110 min using a wet transfer apparatus (Bio-Rad).Western blots were blocked in 5% nonfat milk in Tris–buffered saline with 0.1% Tween-20 (TBST) and 1% normal goat serum for 1 hour. Blots were then incubated with polyclonal rabbit-anti-NR1 primary antibodies diluted [Chemicon, 1:200] in TBST and 1% normal goat serum for 2 hours. Blots were then washed 3 x 15 min in TBST and incubated with horse-radish peroxidase (HRP)-conjugated goat anti-rabbit secondary antibody (Jackson Laboratories) for 1 hour at 1:10,000 in TBST and 1% normal goat serum. Chemilluminescence (Amersham) was used for detection of bound primary antibody. Microsomes isolated from C57 Bl/10 total skeletal muscle via a previously described method were utilized as a positive control [**48**].

Fiber Type Analysis

Fiber type differentiation was assessed via β-nicotinamide adenine dinucleotide [reduced form] (NADH) staining. 8 µm quadriceps sections of C57 Bl/10 mice aged 1 day, 1 week and 1 year were incubated at 37°C for 30 minutes in NADH stain (0.2 M Tris [pH 7.4], 1.5 mM NADH disodium salt [Sigma], 1.5 mM nitro-blue tetrazolium [Sigma]). Sections were then rinsed for 2 minutes each in 30% acetone, 60% acetone, 90% acetone, 60% acetone, and 30% acetone sequentially and successively. Samples were mounted in Crystal Mounting Medium. Images were taken through a Nikon Eclipse 800 epifluorescence microscope using a SPOT-RT slider digital camera and Spot® software.

RNA Isolation and RT-PCR

C57 Bl/10 mouse diaphragm was dissected to enrich for NMJs by excising muscle tissue around the phrenic nerve. Total RNA was isolated from both NMJ-enriched

skeletal muscle and brain tissue using the TRIzol reagent (Invitrogen), according to the manufacturer's directions. Briefly, skeletal muscle tissue collected from hindlimbs and was homogenized with TRIzol reagent at 1 mL per 50-100 mg tissue. Chloroform was added at 0.2 mL per l mL Trizol and aqueous phase was removed from mixture. Isopropyl alcohol was added to precipitate RNA. The resultant RNA pellets were washed with 75% ethanol (aq) and resuspended in distilled water. RNA was then assessed for purity and quantified on a UV Spectrophotometer (Beckman Du-64) at 260/280 nm. To eliminate DNA and protein contamination, 5 µg RNA was treated with Proteinase K (50 µg/mL; Invitrogen), RQ1-DNase I (1 mg/mL; Promega) and RNase Out™ (40 U/µl; Invitrogen) for 20 minutes, then extracted via phenol-chloroform method. Elimination of DNA contamination was confirmed by PCR of treated RNA. To produce cDNA, the SuperScript™ III First-Strand Synthesis System for RT-PCR (Invitrogen) protocol was followed: 2 µg of purified RNA was mixed with 0.8 µl random hexamers (50 µM stock), 0.2 µl Oligo-dT (50 µM stock), 1 µl dNTP mix (10 mM) and DEPC-treated water in a final volume of 10 µl. The mixture was heated to 65°C for 5 min, and then chilled on ice for 2 minutes. The first strand cDNA was synthesized in the following buffer: 2 µl 10X RT buffer, 4 µl $MgCl_2$ (25 mM), 2 µl DTT (0.1 M), 1 µl RNase Out™ (40U/µl), and 1 µl Superscript III (200 U/µl), a reverse transcriptase at 25°C for 10 min followed by 50°C for 50 min, followed by 85°C for 5 min then stored at 4°C. cDNA presence and purity was assessed via PCR utilizing control primers capable of only producing a product from cDNA.

PCR Analysis

Purified skeletal muscle cDNA was analyzed by PCR using primers specific for the receptors of interest. The NCBI Database was used to download cDNA gene

sequences for NR1, NR2A, NR2B, GluR1, GluR2 (both known splice variants, *a* and *b*) and GluR3. Primers were designed against these sequences using MacVector (Accelrys) for primer integrity and are described in *Table 2-2* and *Figure 2-1*. All reactions were carried out for 35 cycles with specifics for each primer shown in *Table 2-2*. For PCRs with extension times less than three (3) minutes, Bullseye Long Taq Polymerase (MidSci) was utilized. For PCRs with extension times longer than (3) minutes, *Pfu*Turbo® Polymerase (Stratagene) was utilized. Purified brain cDNA and mouse genomic DNA were utilized as a positive and negative control, respectively. A water-only control was utilized as a template control.

Sequencing

PCR products from the "pan region" of the NR1 gene (*Figure 2-5* in Results section) were cut from a 1% agarose gel. To remove excess agarose, products were placed in a 600 µl microcentrifuge tube containing glass wool which was suspended above a 1.5 ml microcentrifuge tube. Tubes were centrifuged at 14,000 rpm for 20 min and the 600 µl microcentrifuge tube containing the glass wool was separated out from each 1.5 ml tube. PCR product was then purified by adding 3M Sodium Acetate (1:10) and 100% ethanol (2.5:1). The resulting DNA pellet was washed with 70% ethanol and allowed to precipitate for 72 hours, before being resuspended in 15 µl TE Buffer. Concentration and purity of DNA were recorded using the Nanodrop® 2000 (Fisher Scientific). DNA was sequenced (Genewiz, Inc., North Brunswick, NJ) using the reverse primer for the NR1 "pan region" (*See Table 2-2*). Mouse genomic DNA isolated from a tail biopsy of a C57 Bl/10 mouse was used as a control.

Table 2-2

Gene	Forward Primer	Reverse Primer	Annealing Temp (°C)	Extension Time (m:s)	Expected Product Size (bp)
NR1 (full)	5'-CTAGTGTATTACATCCCAACTG-3'	5'-ACGAGACTAGTGAGACGTGC-3'	56	2'00"	2648
*NR1 N1 Cassette**	5'-TGACATTCGCCCTGCTTTTC-3'	5'-CTCGTTCTTGCCGTTGATTAGC-3'	61	1'00"	812
*NR1 "Pan Region" **	5'-TCAACGGCAAGAACGAGTCG-3'	5'-ACAGTGTGCTCTGAAAGGGCTG-3'	59	1'00"	873
*NR1 C1+C2 Cassette**	5'-TGGAACGGAATGATGGGAGAGC-3'	5'-CGGCAGCACTGTGTCTTTTTGG-3'	59	1'30"	1263
*NR1 C1+C2' Cassette**	5'-GCAACAAAAAGGAGTGGAACGG-3'	5'-CAGCGTCTGAGGAAGCCTATTG-3'	60.5, 61**	2'00"	1941
NR2A	5'-GCTACTGGACCTTGCTGGTATTGC-3'	5'-GCTGTCATTTACTGCCTGTGATGG-3'	51, 53**	4'40"	4184
NR2B	5'-TCTTCTGTCCCTTTATCCTCCGTC-3'	5'-CAAATGTCCTTCTGGAAACGTACC-3'	59	4'40"	4477
GluR1	5'-GGACCAGGGCTTCTTTTTCG-3'	5'-GCGGTGTTTCATTTCTTTGTTTTTG-3'	59	3'00"	2856
GluR2a	5'-AAGGAGGAAAGGGAAACGAGG-3'	5'-CGGAACCAAACCAAAGCCTG-3'	56, 58**	3'00"	2541
GluR2b	5'-TCATCATCATCTCCTCCTACACGG-3'	5'-GCCTCTCACCACTTTGACAATAAAC-3'	57, 58**	3'00"	999 or 652
GluR3	5'-CGGGCGGTGTTCTTTTTACTCC-3'	5'-CACCAAGGAGAGTGAAATCTGGC-3'	57, 59**	3'00"	2753

Table 2-2. Primers for RT-PCR analysis of Glutamate Receptors. Primers were ordered from Sigma Genosys and were used at 100 ng/µl.
* PCRs were performed for 40 cycles in lieu of standard 35 cycles.
** PCRs for brain cDNA did not yield reaction products as expected.

Figure 2-1

A.

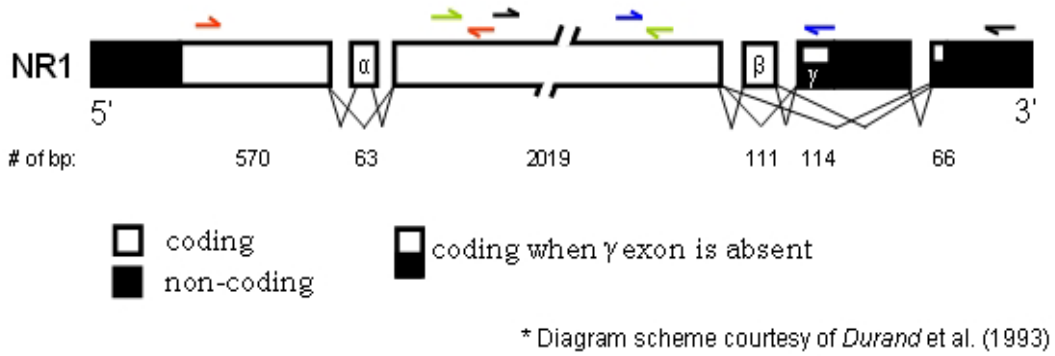

B.

Primer Name	Color	Forward	Reverse	Exons incorporated
N1	Red	21 bp from 5' start codon (including start codon)	1191 bp from 3' of "Pan region"	α
Pan	Green	813 bp from 5' of "Pan region"	333 bp from 3' of "Pan region"	
C2	Blue	1491 bp from 5' of "Pan region"	63 bp from 3' end of coding sequence of γ exon	β, γ
C2'	Black	906 bp from 5' of "Pan region"	894 bp towards 3' end, in a non-coding region; only codes if γ exon is absent	β

Figure 2-1. RT-PCR design, showing amplification strategy and primer locations in relationship to known alternatively spliced exons in brain. (**A**) Four regions were amplified and then sequenced: the N-terminus (N1), a "Pan" region common to all isoforms (Pan), and the C-terminus, dependent upon alternative splicing (C2, C2'). Brain cDNA was utilized as a positive control. (**B**) Chart indicating the exact starting and stopping of the primers along the NR1 gene. Each primer is designed to incorporate certain splice-variant exons, except the "Pan" primer, which is designed to detect all isoforms present.

Results

Immunofluorescence and NADH staining reveal that NR1 localizes to the NMJ coincident with fiber-type differentiation.

Immunofluorescence of mouse quadriceps aged 1 day, 1 week and 1 year revealed that NR1 localized to the NMJ between 1 day and 1 week after birth. Concurrent NADH staining of serial sections showed that fiber-type differentiation occurs within the same timeframe (*Figure 2-2*). Specificity of the NR1 antibody was tested by western blot analysis, which revealed a single band at ~120 kDa, consistent with literature values for the NR1 subunit (*Figure 2-3*). We additionally tested the NR1 antibody on muscle-membrane proteins (microsomes), which are optimal for antibody binding to an NR1 epitope within the context of cellular membranes. Microsomes also showed NR1 antibody binding at ~120 kDa.

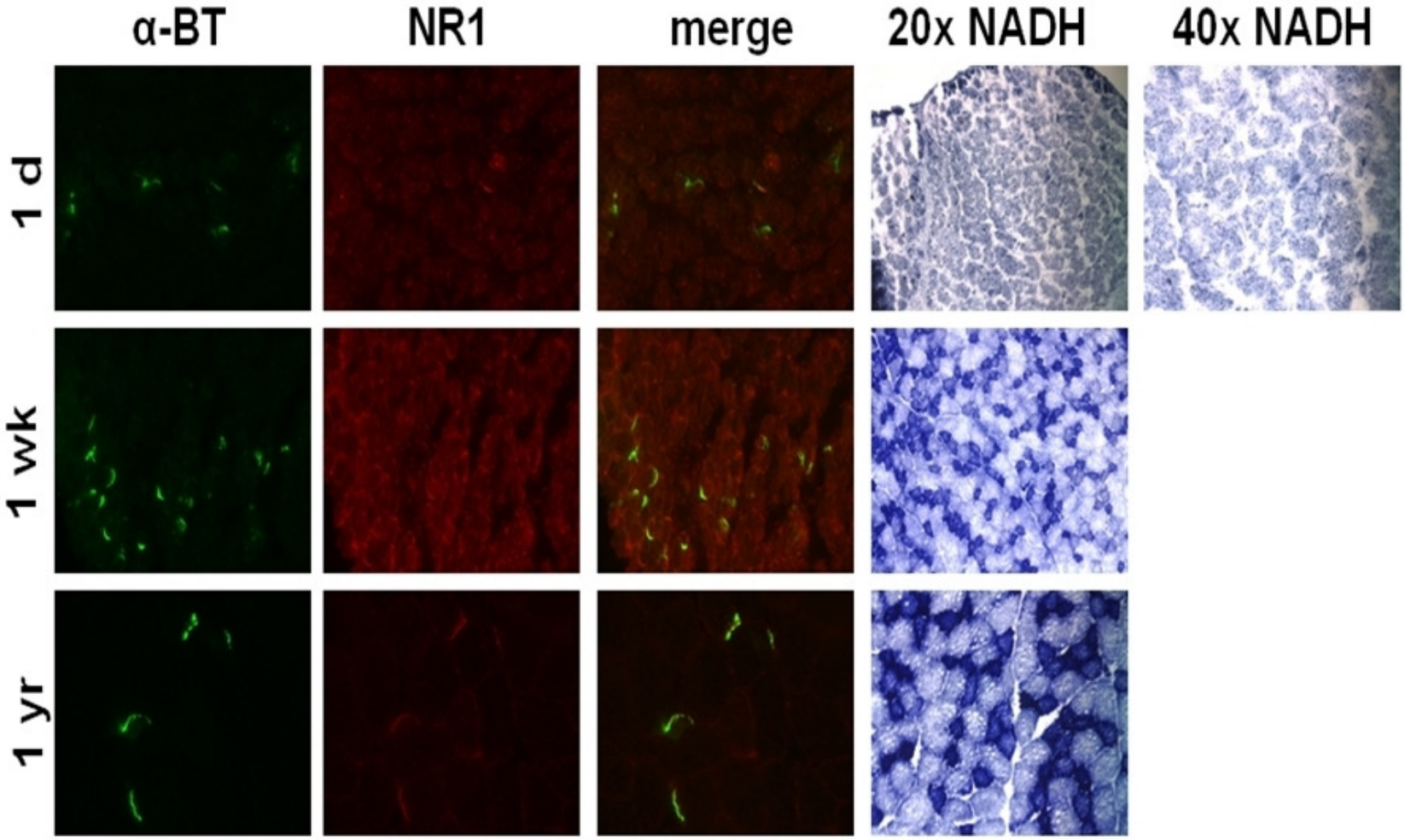

Figure 2-2: Immunofluorescence of NR1 on C57 Bl/10 unfixed quadriceps of mice aged 1 day, 1 week and 1 year. Green indicates localization of acetylcholine receptors (Alexa 488-conjugated α-BT adherence); Red indicates CY3-labeled anti-NR1 antibody. Right columns are NADH staining of oxidative (dark) and glycolytic (light) fibers. (40X NADH is shown to illustrate no definitive fiber-type differentiation at 1 day post-natally).

Figure 2-3

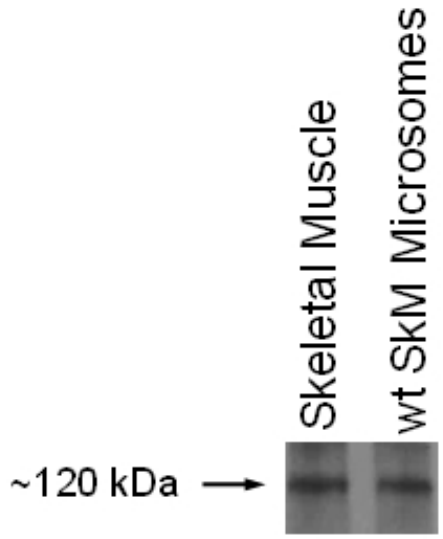

Figure 2-3: Western Blot analysis of NR1 on skeletal muscle and skeletal muscle microsomes. Bands at ~120 kDa are consistent with NR1 isoform sizes found in brain [**31, 69**].

Amplification of NR1 "pan region" cDNA reveals possible alternative splicing of NR1 in skeletal muscle.

RT-PCR of isolated total skeletal muscle RNA (purified to remove genomic DNA) yielded skeletal muscle cDNA. To confirm that cDNA was isolated, PCR was performed using primers for the *dystrophin* gene that bind to exon sequences across large introns in genomic DNA (*Figure 2-4*). Using the purified and verified cDNA, we performed PCR used primers shown in *Table 2-2* to amplify glutamate receptors and regions of the NR1 gene. Despite numerous attempts at optimizing the PCR reaction (i.e. adjusting annealing temperatures and extension times), 5 of the 11 the primer sets (to amplify NR1 (full), NR1 C-termini regions, NR2A, GluR2 (both isoforms) and GluR3) failed to produce reaction/PCR products from skeletal muscle and brain control cDNA. Primers for the NR1 N1 Cassette, NR2B and GluR1 receptors all showed positive bands for brain control, but did not show bands in skeletal muscle cDNA (*Figure 2-5A*). Interestingly, only one primer set, specific for the NR1 "pan region", yielded two bands

in skeletal muscle (*Figure 2-5B*) and brain control (data not shown). A PCR product was also generated from the genomic DNA, even though the primers bound to different exons. The two bands from skeletal muscle were separated, purified and their nucleotide sequences determined (*Figure 2-5C*, *Figure 2-6A, Figure 2-6B*).

Figure 2-4

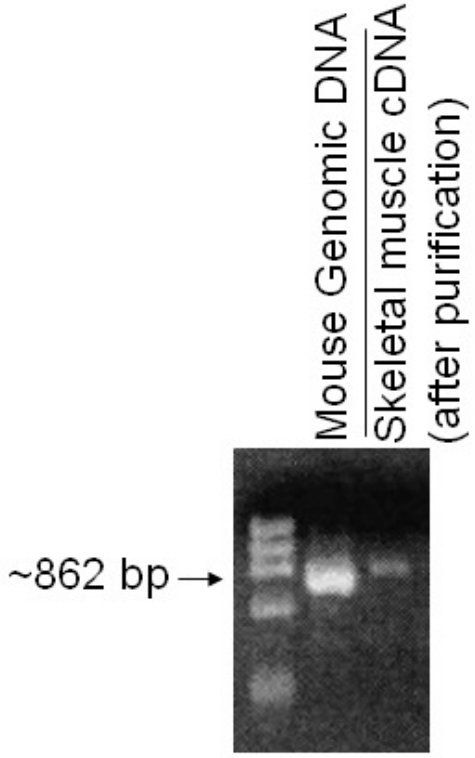

Figure 2-4: Results of RT-PCR from skeletal muscle and brain cDNA. Primers for *dystrophin*, a protein abundantly expressed in skeletal muscle were used to verify the presence of cDNA.

Figure 2-5

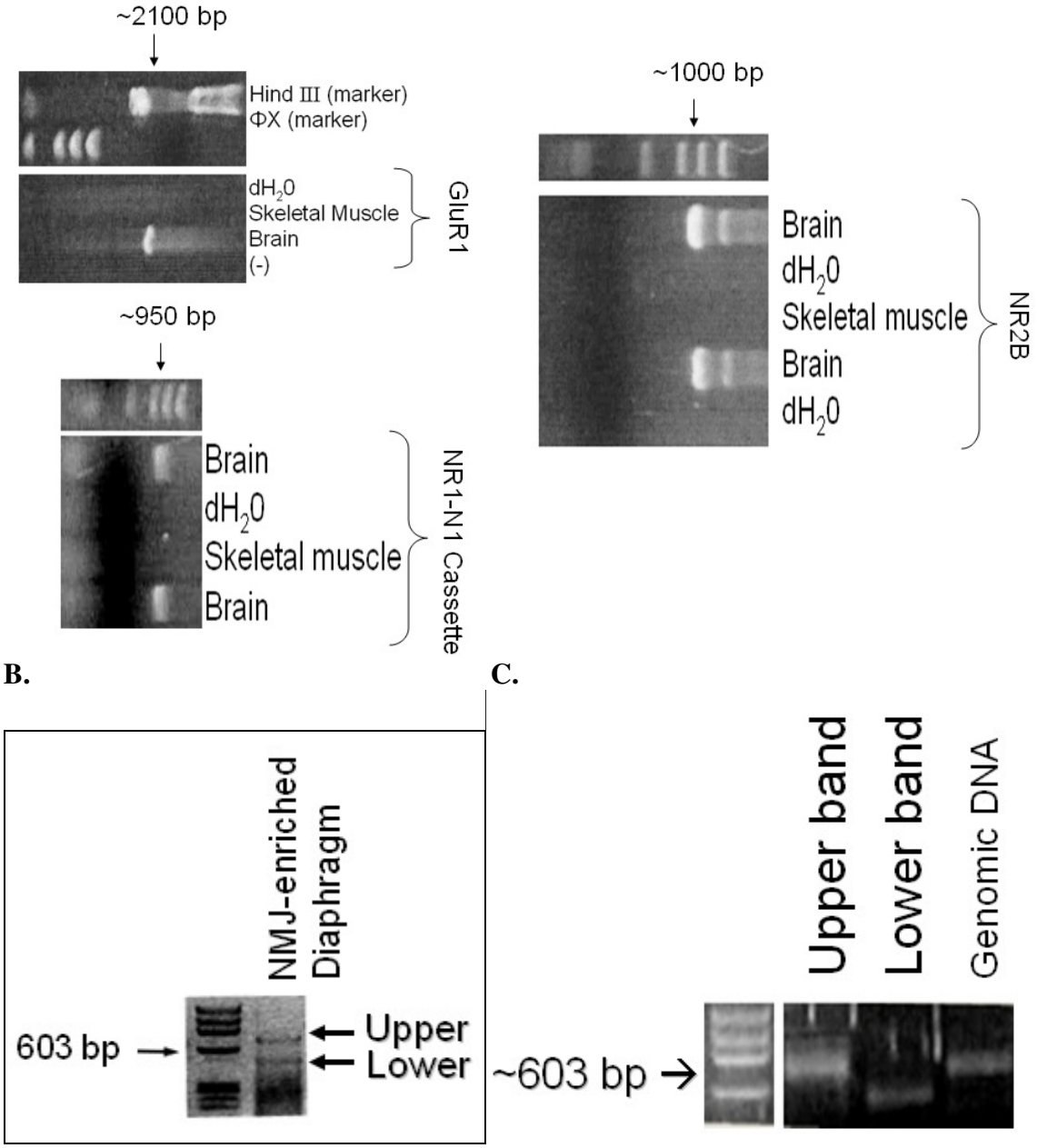

Figure 2-5: Results of PCR from skeletal muscle and brain cDNA using glutamate receptor subunit primers designed as shown in *Table 2-2*. (**A**) Brain cDNA (positive controls) produced bands on PCR with GluR1, NR2B and NR1-N1 Cassette primers. (**B**) NR1 "pan region" primers revealed two bands in skeletal muscle cDNA at approximately 700 bp and 550 bp in size. (**C**) Bands from the positive NR1 "pan region" primers were isolated, separated and purified.

Sequencing revealed dual sequences for the NR1 lower band and were inconclusive for the upper band (*Figure 2-6*). The lower band was found to be composed of a complex mixture, with all unknown bases often showing strong peaks for two bases on chromatogram (*Figure 2-7*). When aligned with known mouse cDNA using MacVector®, a strong homology was displayed (*see* **Appendix A** *at end*).

Figure 2-6

(A)

Sequence File : 15A-1_2710A_1-14-09-NR1-Pan-1780R.seq

>15A-1_2710A_1-14-09-NR1-Pan-1780R_B12.ab1
CATNAGNNGAGCGTATAATCCCTCTGCTACGGCAAGNAAGTGCACCTGTCAACATAAAGCTGTCGNNTGANAGAGCNCCT
TTTACANGAACTGTNCGACCGATATGGTGCTCNCATCNTNCNNATAATTNGNCCAAGGTCACNNATTGGANTNTNACCNN
ATANNACACGTGACTCTATAGGCCTGTNAGNNCCTGGGCNTGGCCGNATGCNATGANGCTNNCCACGCTTNNGTNGNGTN
GCTCTCACTGNCCGCTTTCCAGTCGGGAAACCTGTCGTGCCAGCTGCATTAATNAAACGGCCNAAGNGCGGGGAGTAGAC
GGTTTGCGTATTGGGCGCTCTTCCGCTTCCTCGCTCACTGACTCGCTGCGCTCGGTCGTTCGGCTGCGGCGAGCGGTATC
AGCTCACTCAAAGGCGGTAATACGGTTATCCACAGAATCAGGGGATAACGCAGGAAAGAACATGTGAGCAAAAGGCCAGC
AAAAGGCCAGGAACCGTAAAAAGGCCGCGTTGCTGGCGTTTTTCCATAGGCTCCGCCCCCCTGACGAGCATCACAAAAAT
CGACGCTCAAGTCAGAGGTGGCGAAACCCGACAGGACTATAAAGATACCAGGCGTTTCCCCCTGGAAGCTCCCTCGTGCG
CTCTCCTGTTCCGACCCTGCCGCTTACCGGATACCTGTCCGCCTTTCTCCCTTCGGGAAGCGTGGCGCTTTCTCATAGCT
CACGCTGTAGGTATCTCAATTCNGNNGTAAGGTCGNTTCGCTCCAAGCTGGGGCTGTGTTGCANNAAACCCCCCNCGTTC
ANCCCGACCGCTGCGACTTATCCGGNAAACTATNGTCTTGNNTNCCAANCCNGGTAANANCNANTTTNNNNCANTGGCAN
CAANCCNCTGGTAAANGATTAANNANAACNNAGGTANNGTNANGCGGNGCCNACNNNAANTTNNNTGNAANTGGTGGNNC

(B)

Sequence File : 6_Hex_B_12-23-08-NR1-Pan-1780R.seq

>6_Hex_B_12-23-08-NR1-Pan-1780R_G11.ab1
TTTGNNNAACNNTANTAANNANGTCTNTNAAAGNCCTAAAAAGCCTCTNTAAGGGCCNAAAAAGAGGTTTTTANCCCTTT
NAAAAAGAGNNGACAAGCATACNAAAACATCNNTGAAAANANTNAANGACGTGGATCNNTGGGACNGNATACNGATGTNG
GGNCCCGGNTCCNTGGCNNACNGTGNTGGTNCNCGCANGGNGGAGCCAAANCGGAGCNNAAAGCCTTGCGCNCACTGCCN
CCGTNCTCAGNGGGGAACNTCNCNCTGCANGGCNGACATTGNNCANGCNNGCGGGATCCGANGGGAAGATGCCNGATCGN
AANACANGGNTCGNTCGCNCGCGCGGTCGCNGCCAGTCNCNNCCNCNANTNNCCAACGGTAGTNACNGCNGNGGCGANGG
NGNNGAGCTGANGCNCNNGCNGCACTACCGTNGNTCNCCTTAATAANGGTGCTACGCCCGCAGCNANANGCGNGCNAACG
NGNCCCTNCNGGCCTTGGNGANGGNCCAGGNCGATCNCGCTGGGCTTNGNCNTANNTGTGNCAGNGGCGGTGCCGGGNGG
NGCATGGCGAGACGCTNNNGAGGAGCTGTGTCNCNGNGNTGGCGCNANTCCNGTGNCATCAGGCACGGCCNCNCTGCAAG
CCNCAACNTNNGNGGGNCNNGGCCAGGCTGAGGCCNATGCCGCCATNCNTNANGCTNNTNCTGNCNNNNGGCAGCANTNN
CGGNANTTGTCCGNGCNCCGGNCACGCNCCNCNNTGTNCCGNNCTGNNGTTTCNNGGGNGCNATGNNNACNANTCNTGNN
AACCNCANCCNCANTNNCTGGTNCNCNACTTCNNNCNAAGGNNCCTCCCNNNGCGCCGAAGGGNNNACNTTCGTCTGAAN
NNTGATCAATTCTNTCGTCAANNGNCNNCCAGGCCNNNGNANCAGCNCCCCGGNGGCCGAANGGCGGGNGNCTTCATNNG
GGNGTAAAGGCNNGGNNGNANCCCCNATCCANNGCTNNNGGGGGNCNNNCAACCCNTANGGGANGANNGGGANNCCNTNT

Figure 2-6: Results of sequencing from Genewiz®. (**A**) Sequence produced from the lower band isolated in *Figure 2-5C.* (**B**) Sequence produced from the upper band isolated in *Figure 2-5C.* "N" indicates unknown bases.

Figure 2-7

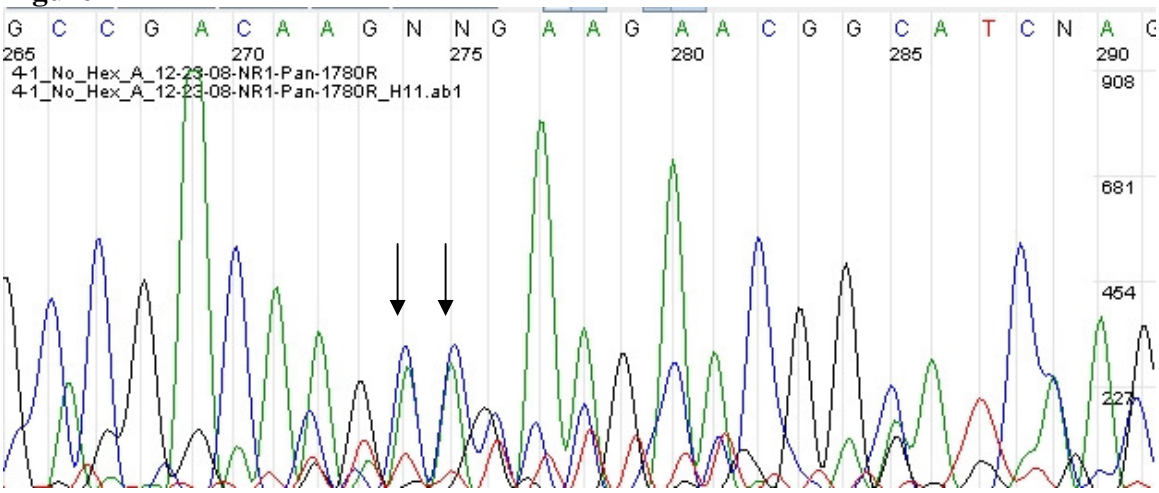

Figure 2-7: Some peaks on chromatogram for the lower band show strong dual peaks, suggesting this might be a complex mixture of cDNA. Arrows indicate possible alternative peaks. Representative sample shown (Genewiz).

Discussion

The data presented herein suggest that NR1 localizes to the NMJ between one day and one week after birth, and is maintained there at 1 year of age. Of particular interest, NADH staining (*Figure 2-2*) confirms that between 1 day and 1 week is also the approximate timeframe when skeletal muscle fibers are differentiating. Combined, these results offer evidence that NR1 is present during fiber-type differentiation. It also opens up the possibility that NR1 contributes to fiber-type differentiation. However, as functional NMDA receptors require both NR1 and NR2x subunits, similar experiments to assess the expression of NR2A and NR2B subunits need to be conducted in order to test whether complete functional receptors are associated with fiber-type development. If we are able to show that the timing of NR1 and NR2A/B expression were concurrent, we could then ask the question: are they complexed together between 1 and 7 days post-birth. Our lab has only demonstrated that NR2A and NR2B are both present at 5 weeks of age in the mouse NMJ [**38**]; the time period of 1 day to 1 week has not yet been assessed.

While we cannot guarantee the antibody specificity for NR1, the western blot of NR1 (*Figure 2-3*) is in agreement with previous literature reports for NR1 protein size at ~110-120 kDa. However, we did not run the proper controls on that particular western blot (*Figure 2-3*)—that is, no negative control or brain homogenate (positive) control were included for comparison. Though the protein bands appear at the proper size without other bands present, we cannot conclusively state based on this data alone that the NR1 antibody is not cross-reacting with another similar amino acid sequence. Of note, finding an anti-NR1 antibody has been a cumbersome task. We tried at least four commercial anti-NR1 antibodies (both poly- and monoclonal) for western blot and immunofluorescence optimization. Shown are the best examples of these trails.

The second goal of this study was to identify which isoforms of NR1 were present in skeletal muscle. To do this, we isolated RNA from NMJ-enriched skeletal muscle and reverse-transcribed to generate the expressed DNA (cDNA). We then used primers specific for glutamate receptors and NR1 regions to amplify the regions in the purified cDNA and determine whether they were expressed at the NMJ. Only a single region—the region common to all known NR1 protein isoforms—was amplified, confirming that NR1 is expressed in skeletal muscle.

There are several possible reasons why the other primers failed to amplify the receptors or NR1 regions that they were designed to detect. First, as with any primers, a fair portion of "guess work" is required to optimize conditions in which the PCR will be successful. Suggested annealing temps are provided when the primers are designed and ordered based upon their size and composition of the primers. Extension times are estimated at approximately 1 minute for every 1 kb sequence to be amplified. Even with

these general guides, many primers do not bind based upon formulae and estimations. It is possible that with the primers designed, additional reaction optimization would yield PCR products. Regrettably, there was not enough time for further testing.

Secondly, fewer mRNA transcripts of glutamate receptors are present in skeletal muscle. The bulk of muscle is major proteins that are hundreds of kiloDaltons in size: actin, myosin and tropomyosin. For a small protein found solely at the NMJ, amplification of mRNA transcripts for NR1 specificially might prove arduous given that RNA isolation and cDNA creation techniques would amplify to all RNA sequences expressed. However, ACh receptor mRNA has successfully been amplified from skeletal muscle [**29**] and presumably would be as rare of a transcript as NMDA receptor subunits given where it is expressed solely at the same junction in skeletal muscle. Thus, it is completely plausible that, with further optimization, future glutamate receptor identification using specific primers can be successful.

One concern might be that the failed primers were simply poorly designed. It is possible that the forward and reverse primers cross-reacted, or that the difference of annealing temperatures between forward and reverse primers was too great. However, for three primer sets (NR2B, GluR1 and the NR1-N1 Cassette), the positive control (brain) worked well (*Figure 2-5A*), eliminating this concern. The brain PCR product bands for each of these primers appeared at expected sizes (*Table 2*-2, *Figure 2-5A*). For these three sets, perhaps further amplification of the skeletal muscle samples (using PCR to re-amplify the PCR product mixture) or amplification with a more efficient *taq* polymerase might have provided bands. When a positive band for the NR1 “pan region” was identified, the focus was shifted to identifying the sequence of that band.

Based upon sequencing data, our hypothesis that multiple splice variants of NR1 are present in skeletal muscle was supported. The dual bands from RT-PCR (*Figure 2-5B*) are of different sizes from those shown in the genomic DNA controls, and also differ from the brain control (data not shown). After separation and sequencing, the lower band revealed dual gene sequences with strong homology to mouse NR1 (*Figure 2-7*). The upper band did not produce viable data; however its band is particularly strong on gels (*Figure 2-5C*). We conclude that the poor quality of isolating this band—possibly due to agarose contamination of the sample during gel purification—has left its sequence indeterminate for the time being. Further efforts to purify this band may yield a usable sequence for comparison to known NR1 gene splicing. However, before any further conclusions might be made regarding NR1's function in the brain a definitive answer as to the sequencing homology between isolated skeletal muscle cDNA and known NR1 sequences must be clarified.

The data presented here lay a foundation for challenging the dogma of the "simple synapse" of the NMJ; however, identification of NR1 expression in skeletal muscle is not sufficient. It is possible that these receptors, although present, are non-functional; to reach a conclusion, we must directly test functionality.

III

Physiological Role of Glutamate Receptors in Normal Murine Skeletal Muscle

Introduction

From an evolutionary perspective, it is unlikely that the presence of glutamate receptors would be maintained if they were not physiologically relevant. Certainly an argument can be made regarding vestigal traits and structures, but we cannot rule out the possibility of functional relevancy. Research in brain tissue has overwhelmingly defined the roles of NMDA and AMPA receptors in terms of mental conditioning, learning, intercellular signaling, long-term plasticity and other memory mechanisms, psychiatric and neurologic disorders and toxicity. In skeletal muscle, however, most of these functions are neither plausible nor relevant. Glutamate receptors are unlikely to be directly involved in skeletal muscle contraction due to ACh functioning as the key neurotransmitter. Therefore a new question is raised: are these receptors functional at the NMJ?

To address this question, we must consider how skeletal muscle functions in conjunction with the nervous system. Nerve impulses are propagated along a neuronal axon to the axon hillock, where depolarization of the membrane causes the axon terminal to become permeable to Ca^{2+}. As Ca^{2+} rushes into the axon terminal, vesicles containing neurotransmitters fuse with the cell membrane towards the synapse, and their contents are released into the synaptic cleft. In skeletal muscle, the classical neurotransmitter is ACh. When ACh binds to its receptor along the primary folds of the NMJ, a Na^+/K^+ channel is opened, to which Na^+ rushes in and K^+ rushes out. The normal resting potential of -95

mV is maintained by high intracellular K^+ and high extracellular Na^+; when the ACh Na^+/K^+ channel is opened, a depolarization of the resting membrane potential occurs. The depolarization spreads to the sarcolemma-integrated T-tubule system, where it activates L-type Ca^{2+} channels to open and release Ca^{2+}. Ca^{2+} then mediates muscle contraction via binding to the troponin complex and causing actin/myosin/tropomyosin movement.

As with any synapse, the key physiological event is depolarization of the muscle membrane for propagation of the electrochemical signal. As NMDA and AMPA receptors both control ion channels, they are excellent candidates to affect membrane potential. Based on known function of these receptors in brain, we hypothesize that treating myocytes with NMDA and AMPA receptor agonists will stimulate and enhance electrophysiological activity. Conversely, treating with NMDA and AMPA receptor antagonists will disrupt the normal function of the synapse in skeletal muscle. Initially to test this hypothesis, we injected agonists and antagonists directly into mice gastrocnemii, sacrificed them at varied timepoints, and observed for morphological and fiber-type changes. Unfortunately, this pilot experiment failed to produce results due to technical (chemical spreading) obstacles, and we quickly realized that more advanced methods would be in order.

We collaborated with Dr. Luis Polo-Parada, a muscle physiologist at the University of Missouri, one of very few who specialize in single-cell skeletal muscle electrophysiology techniques. Electrical stimulation of the muscle membrane is measured to determine activity of the synapse. At a normal NMJ, neurotransmitter-containing vesicles are released from the axon and depolarize the post-synaptic muscle membrane potential. When one vesicle is released, a very small depolarization occurs; this is

referred to as a miniature end-plate potential (mEPP). In a normal synaptic event, hundreds of vesicles are released synchronously, creating a "build-up" of mEPPs to form a full end-plate potential (EPP). The frequency of mEPPs would therefore indicate the firing of quanta (vesicles) during excitatory synapses. In several disease states, including myasthenia gravis and botulism, the amplitude and frequency of mEPPs is altered, resulting in a decreased end-plate synaptic potential (EPSP) change [**47**]. To test whether NMDA or AMPA receptor agonists and antagonists had an effect on electrical conduction of the NMJ, Dr. Polo-Parada measured the mEPP frequency and Quantal Content (defined as average mEPP amplitude/average EPP amplitude) after various regiments of glutamate receptor agonists and antagonists. Examples of mEPPs and EPPs are shown in *Figure 3-1*.

Figure 3-1

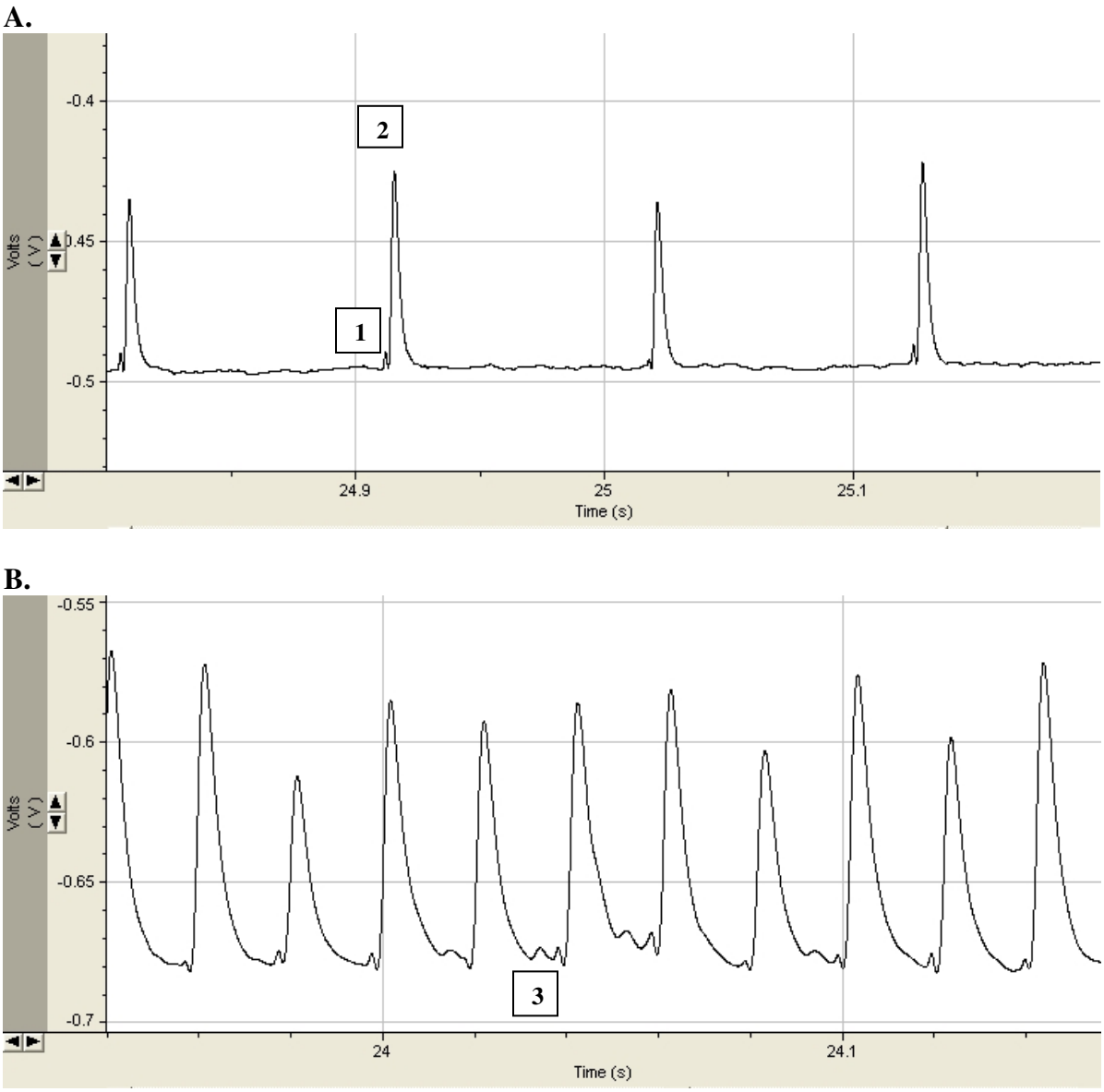

Figure 3-1. Examples of EPPs and mEPPs as recorded on muscle. (**A**) An example of low electrical stimulation in a normal mouse. A single mEPP precedes the EPP (1 & 2 respectively). (**B**) An example of a higher stimulation (increased EPP frequency) after treatment with a glutamate antagonist. Notice how mEPP frequency is greater, indicating more quanta (neurotransmitter vesicles) are being released at the junction (3).

Methods

Electrophysiology

Single-cell electrophysiology experiments were conducted by Dr. Luis Polo-Parada utilizing modified protocols from Dr. Lynn Landmesser's laboratory [**51, 55**]. Semitendinosus muscles from C57 BL/10 mice were excised along with the inserting nerve and perfused with oxygenated Tyrode's solution (125 mM NaCl, 5.37 mM KCl, 24 mM $NaHCO_3$, 1 mM $MgCl_2$,1.8 mM $CaCl_2$, and 5% dextrose containing 1 μM ω-conotoxin GIIIB) at room temperature. In each experiment, glutamate agonists or antagonists were added to the solution to discern changes in mEPPs and EPPs [potential]. The drug regiment is shown in *Table 3-1*. For intracellular recordings of the electrical responses, glass micropipettes (Sutter Instruments, Novato, CA) were pulled with a P-97 Flaming/Brown Micropipette Puller (Sutter Instruments) and filled with 3 M KCl and connected to a Bridge Amplifier BA-1S (npi-Tamm, Germany); a resistance of 60-80 MΩ was used. All recordings were displayed on an oscilloscope (Instek, Chino, CA), digitized in parallel, and stored and processed through a Digidata 1440A under the control of Axotape 10 Software (Molecular Devices Corporation). From each experiment, traces (e.g. *Figure 3-1*) were generated for analysis.

Table 3-1

Experiment #	1st Add.	2nd Add.	3rd Add.	4th Add.
1.A	α-BT	Glu	D-AP5	NBQX
1.B	α-BT	D-AP5	NBQX	Glu
2.A	α-BT	NBQX	D-AP5	Glu
2.B	D-AP5	NBQX	Glu	α-BT
3.A	D-AP5	NBQX	α-BT	Glu
3.B	D-AP5	Glu	NBQX	α-BT
4.A	NBQX	Glu	D-AP5	α-BT
4.B	NBQX	D-AP5	α-BT	Glu
5.A	Glu	D-AP5	NBQX	α-BT
5.B	Glu	NBQX	D-AP5	α-BT

Table 3-1. Experiments determining physiological effects of glutamate agonists/antagonists at the NMJ. In each experiment, several drugs were added to a single muscle cell in the order prescribed (1st add, 2nd add, etc.) at 10-15 second intervals. Each experiment yielded different types of data; for example, Exp. 1.A determined if glutamate can act as a functional neurotransmitter if ACh receptors are blocked with α-BT. **Glu** = Glutamate, broad ionotropic glutamate receptor agonist; **D-AP5** = D-2-amino-5-phosphonopentanoate, NMDA receptor-specific antagonist; **NBQX** = 2,3-dihydroxy-6-nitro-7-sulfamoyl-benzo[f]quinoxaline-2,3-dione, AMPA receptor-specific antagonist. **α-BT** = α-bungarotoxin, ACh receptor antagonist. All reagents were used at standard concentrations as used in neuronal physiology.

Except for experiments 5A and 5B in *Table 3-1*, I performed all analyses of traces generated by Dr. Polo-Parada using Clampfit 9® Software (Molecular Devices Corporation). Traces contained both EPPs and mEPPs (*Figure 3-1*), and all mEPPs and EPPs were measured for amplitude and recorded by the Clampfit program. Measurements were then recorded in an Excel® table and statistical analyses were conducted using Excel® (Microsoft Corporation). Average mEPPs, average EPPs, quantal content (QC), frequency of mEPPs and relevant statistical testing for significance (*t*-test, standard error) were all determined.

All experiments designed in *Table 3-1* were conducted by Dr. Luis Polo-Parada. However, not all traces that he generated could be analyzed. The data for the files that were analyzed can be found in *Table 3-2*.

Table 3-2

Trace #	DURATION (s)	AVG. EPPS	AVG. MEPPS	MEPPS FREQUENCY (ms^{-1})	QC	Treatment
2008-07-14-0001	29.107	0.069069	0.004688	0.011956	14.73318	Control
2008-07-14-0004	44.39	0.057983	0.004931	0.007051	11.75827	Control
2008-07-14-0006	25.309	0.058353	0.003259	0.004899	17.90596	Control
2008-07-14-0008	25.86	0.050157	0.00529	0.016009	9.481078	DAP-5 alone
2008-07-14-0010	26.317	0.02184	0.004996	0.011779	4.371288	DAP-5 alone
2008-07-14-0013	47.667	0.01114	0.004229	0.000462	2.634061	DAP-5 alone
2008-07-14-0015	42.19	0.098109	0.004456	0.008628	22.01888	DAP-5 alone
2008-07-14-0018	44.95	0.184926	0.004509	0.008966	41.0156	DAP-5 then NBQX
2008-07-14-0020	39.89	0.201143	0.00359	0.015618	56.03549	DAP-5 then NBQX
2008-07-14-0024	26.655	0.163412	0.00804	0.015082	20.32393	DAP-5 then NBQX
2008-07-14-0025	26.705	0.149879	0.005969	0.017263	25.11142	DAP-5 then NBQX
2008-07-14-0028	29.184	0.067679	0.002836	0.020148	23.86235	Control prep 2
2008-07-14-0030	32.205	0.056845	0.002443	0.020432	23.26483	Control prep 2
2008-07-14-0031	26.521	0.049445	0.002146	0.006523	23.04517	Control prep 2
2008-07-14-0034	32.256	0.223502	0.010849	0.004495	20.60076	Glu/Gly added (alone)
2008-07-15-0000	26.63	0.058882	0.003694	0.01611	15.94077	Control prep 3
2008-07-15-0002	25.65	0.055864	0.002021	0.015634	27.64481	Control prep 3
2008-07-15-0004	12.391	0.067242	0.001519	0.000242	44.27716	Control prep 3
2008-07-15-0007	51.31	0.01211	0.001702	0.003138	7.11456	Control prep 3
2008-07-15-0009	56.61	0	0	0	0	a-BTx then DAP-5
2008-07-16-0000	29.42	0.121384	0.014382	0.014344	8.440037	Control prep 4
2008-07-16-0002	32.31	0.108773	0.007639	0.012659	14.23961	Control prep 4
2008-07-16-0004	27.81	0.186304	0.00874	0.015067	21.31586	NBQX alone
2008-07-16-0009	75.11	0.035829	0.010673	0.000612	3.356953	NBQX then Glu/Gly
2008-07-16-0011	36.05	0.014679	0.002884	0.015756	5.089986	NBQX then Gly/Gly then DAP-5
2008-07-16-0013	28.674	0.04537	0.010768	0.011299	4.213261	Control prep 5
2008-07-16-0014	11.504	0.052262	0.001282	0.013908	40.77036	Control prep 5
2008-07-16-0016	26.7	0.040291	0.003332	0.013071	12.09082	Control prep 5
2008-07-16-0020	126.4	0.03133	0.0083347	0.004375	3.759376	DAP5 then Glu/Gly
2008-07-17-0000	29.358	0.122807	0.004347	0.022481	28.24952	Control prep 6
2008-07-17-0003	29.075	0.13094	0.003138	0.013207	41.73364	Control prep 6
2008-07-17-0005	26.16	0.148471	0.005808	0.025726	25.56439	Control prep 7
2008-07-17-0007	28.353	0.029579	0.004926	0.032519	6.005329	Glu/Gly then DAP-5 alone
2008-07-18-0000	25.386	0.048601	0.003204	0.001182	15.16752	Control prep 8

Table 3-2. Electrophysiology measurements of normal semitendenosus muscle. **Duration** refers duration of the entire recorded trace. **Avg. EPPs** were calculated as (Σ EPP amplitudes)/# of EPPs. **Avg. mEPPs** were calculated as (Σ mEPP amplitudes)/# of mEPPs. **mEPP frequency** was calculated as (# of mEPPs)/duration of trace. **Quantal Content** (**QC**) was calculated using the formula (**Avg. EPPs / Avg. mEPPs**). **Treatments** administered are denoted for each trace; "control prep" refers to no treatment. Black bars in the "**Treatment**" column indicated separate the data from different C57 mice.

Results

The data generated from analyzing the physiology traces are listed in *Table 3-1*. Blocking NMDA receptors with DAP-5 alone yielded an increased (but not statistically significant) response in mEPP frequency and a decreased (but not significant) response in QC (red bars, *Figure 3-2*, *Figure 3-3, Figure 3-1B*). However, a nearly statistically significant increase in both mEPP frequency and QC were observed after treatment with the NMDA receptor antagonist, DAP-5, and the AMPA receptor antagonist, NBQX (yellow bars, *Figure 3-2*, *Figure 3-3*).

Figure 3-2

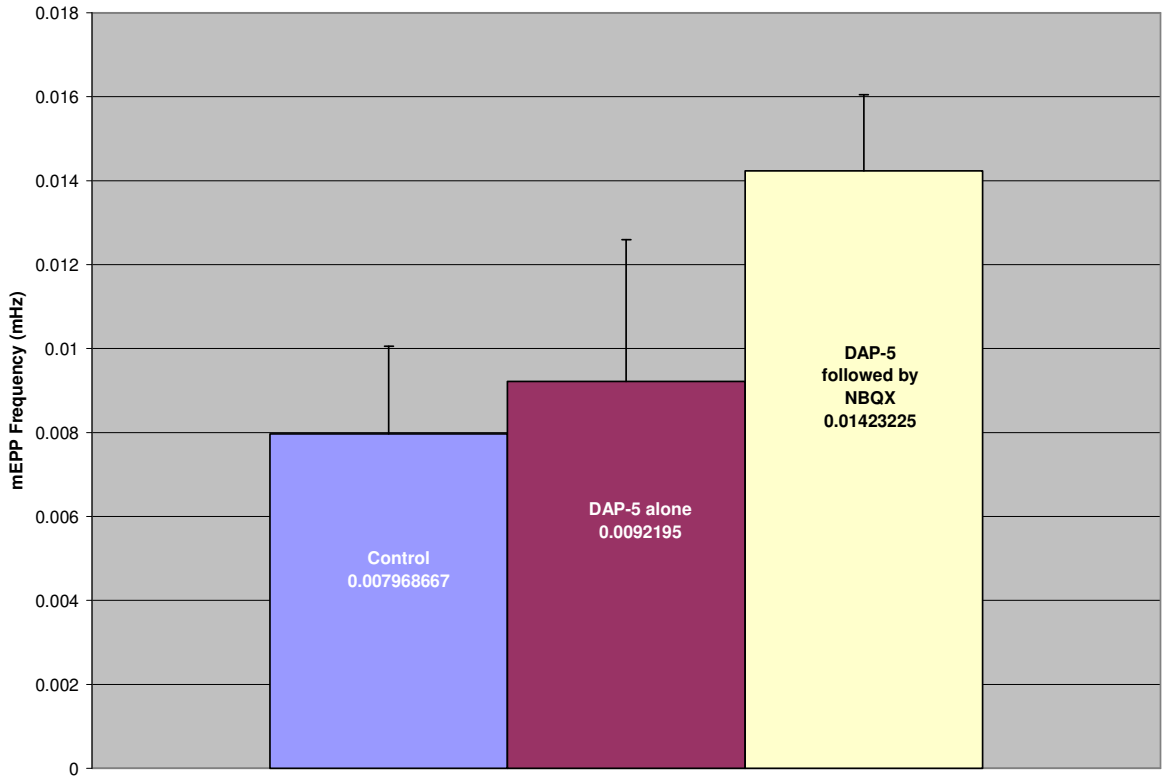

Figure 3-2. Graph showing mEPP frequency from myocytes that were untreated (**Control**), adding an NMDA antagonist (**DAP-5 alone**) and adding two glutamate antagonists (**DAP-5 followed by NBQX**). Significance: **DAP-5** — $p \leq 0.781$; **DAP-5 followed by NBQX** — $p \leq 0.073$.

Figure 3-3

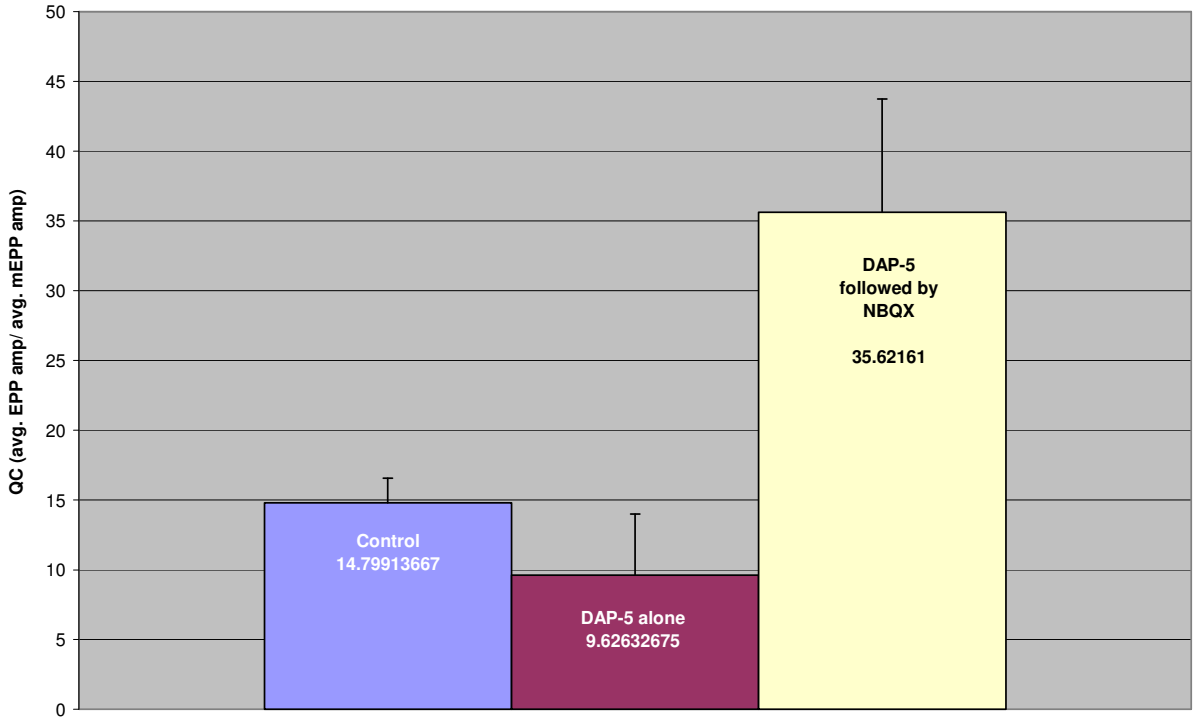

Figure 3-3. Graph showing quantal content from myocytes that were untreated (**Control**), adding an NMDA antagonist (**DAP-5 alone**) and adding two glutamate antagonists (**DAP-5 followed by NBQX**). Significance: **DAP-5** — $p \leq 0.381$; **DAP-5 followed by NBQX** — $p \leq 0.085$.

Due to the fact that sample size was $n = 1$ mouse for all other experiments, statistical analyses could not be conducted. However, it is worth noting that our data in *Table 3-2* are consistent with previous findings that blocking ACh receptors with α-bungarotoxin continues to arrest all action potential propagation at the NMJ (Trace #2008-07-15-0009, where the frequency of both mEPPs and EPPs were reduced to zero). It is also interesting to note that blocking AMPA receptors at the NMJ with NBQX (*Table 3-2*, Trace #2008-07-16-0004) showed an increase in the quantal content released at the NMJ, but did not show a dramatic change in mEPP frequency. When glutamate was added to the system after blocking AMPA receptors, a significant decrease in quantal content occurred (*Table 3-2,* Trace #2008-07-16-0009).

Discussion

Despite the sample size limitation, we were able to discern useful data from the electrophysiology experiments. Blocking the entire glutamate system yields a near-statistically significant increase in both mEPP frequency and quantal content (QC). In other words, vesicles at the NMJ are being released much more frequently and in greater amounts. Perhaps the glutamate system is involved with maintaining normal vesicle release and disruption of this system leads to over-loading of the system. When we blocked NMDA receptors alone, we found no significant change in either QC or mEPP frequency from the controls (p values were significantly high at 0.381 and 0.781, respectively; *Figure 3-2, Figure 3-3*). Consequently, blocking AMPA receptors produced similar results in the single samples in which they were investigated (*Table 3-2*). However, treating the NMJ with glutamate appeared to overwhelm the system and dramatically decrease QC. Increasing the sample sizes for the DAP-5 and DAP-5 + NBQX experiments may allow our findings to reach statistical significance ($p \leq 0.05$).

Blocking ACh receptors at the NMJ arrested all electrical conduction in the muscle. We then attempted to block NMDA receptors to see if we might "rescue" electrical conduction, but this did not occur, suggesting that the muscle glutamate system is electrically-dependent upon action potential propagation to function. We had originally designed an experiment to test whether blocking AMPA receptors would produce the same effect (*Table 3-1*, Experiment 2A), however traces for this experiment were not received/analyzed. Therefore, the role of the glutamatergic system in skeletal muscle with respect to the cholinergic system present there is inconclusive, based upon the studies that we have conducted and analyzed. Further analysis of the other trace files from these

experiments might potentially yield answers to this question, as well as to delineate the specific role of NBQX and DAP-5 at the NMJ. Despite this setback, however, we also tried an additional method by which we would measure function of glutamate receptors—particularly the NR1 subunit—at the NMJ, by removing the protein of interest, and observing phenotypical changes in mice. These experiments are described in *Chapter* IV.

IV

NR1 ablation in Skeletal Muscle is not obtained via the *Cre*-lox mechanism using the HSA promoter

Introduction

The most direct, physiologically-relevant method for testing the function of a protein is to knock out its corresponding gene and analyze changes in phenotype. For several decades researchers have completely knocked-out genes in animals—"total knockouts" (tKO)—and defined functionality of specific genes and their corresponding proteins. However, as genes are often variably expressed in different tissues, the knocking out of a gene in all tissues does not allow for tissue-specific testing of functionality. For example, if a tKO mouse does not survive long enough for further testing, and/or it is known that the protein is expressed in multiple tissues, it is difficult to connect lethality with its role in a specific tissue. Such is the case for NR1, where tKO mice do not feed and die within 10 hours of birth from respiratory failure [**18**]. Further, a tKO model does not necessarily allow for protein function to correlate with gene expression in a particular tissue, as observed phenotypes in one tissue might mask phenotypes observed in other tissues.

In the mid 1990s, a method in which genes of interest might be knocked-out in a tissue specific manner was discovered. This method involved using a well-characterized bacterial recombination system referred to as the "locus of crossover P1" (*loxP*)–Cre recombination system [**68**]. The *loxP*-Cre recombination system requires two *loxP* sites (DNA regions characterized by 8 bp asymmetric sequence flanked by two palindromic 13 bp sequences) on the same chromosome and an enzyme called *Cre* recombinase (*Cre*)

(*Figure 4-1A*). If the loxP sites are inserted in a *cis* fashion (*Figure 4-1B*), *Cre* will specifically cleave within the 8 bp buffer sequence to eliminate a single *loxP* site and any intervening DNA [**23, 45**]. By flanking genes of interest in undifferentiated mammalian cells with *loxP* sites in the presence of *Cre*, Sauer *et al*. demonstrated that gene-specific cleavage can be induced in mammalian cells [**63, 64**]. The *loxP* sites are located in each cell in the organism, but by expressing *Cre* specifically in a tissue of interest; one can eliminate a *loxP* flanked gene (termed "floxed" gene) within that tissue alone. In 1996, Tsien *et al.* designed a flox transgenic mouse line with *loxP* sites flanking the NR1 gene [**71**]. When a homozygous NR1 flox mouse was mated with a mouse with *Cre* coupled to a hippocampal cell gene promoter, Tsien *et al.* successfully excised the NR1 gene solely from CA-1 pyramidal cells in brain.

In this thesis, we sought to determine whether ablation of a glutamate receptor in skeletal muscle would lead to any change in phenotype. This question inherently posed a second question: could NMDA receptor subunits actually be ablated specifically in skeletal muscle? To address these questions, we designed experiments to ablate NR1 selectively from murine skeletal muscle. NR1 was an optimal glutamate receptor subunit candidate for these studies for several reasons. First, NR1 is the obligate subunit; ablating it would render any NMDA receptor complexes dysfunctional. Second, the mice from Tsien *et al.* (NR1 flox) are already developed and maintained by Jackson Laboratories, making them easily accessible for breeding, genotyping and experimentation. Finally, by ablating NR1, we can determine if there is any correlation between NR1 and fiber-type development, as previous data have shown (*Chapter* II—*Immunofluorescence data*). In this study, we will test the hypothesis that absence of NR1 from the NMJ will result in

abnormal skeletal muscle development and maintenance. To test this hypothesis, we will mate these NR1 floxed mice against a muscle-specific Human Skeletal Actin (HSA) *Cre* line, developed by the Melki Lab at the Université Louis Pasteur (Strasbourg, France) [**40**]. The HSA promoter is known to be skeletal muscle-specific and is expressed from prenatal myocyte differentiation [**4**]. From this mating, a conditional knockout (cKO) mouse will be created, in which we will confirm NR1 ablation with immunofluorescence and Western analysis. We will also test cKOs for muscle morphology and fiber-type differentiation at various ages.

Figure 4-1

A.

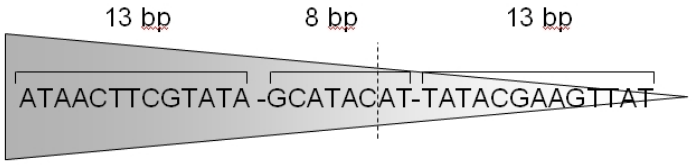

B.

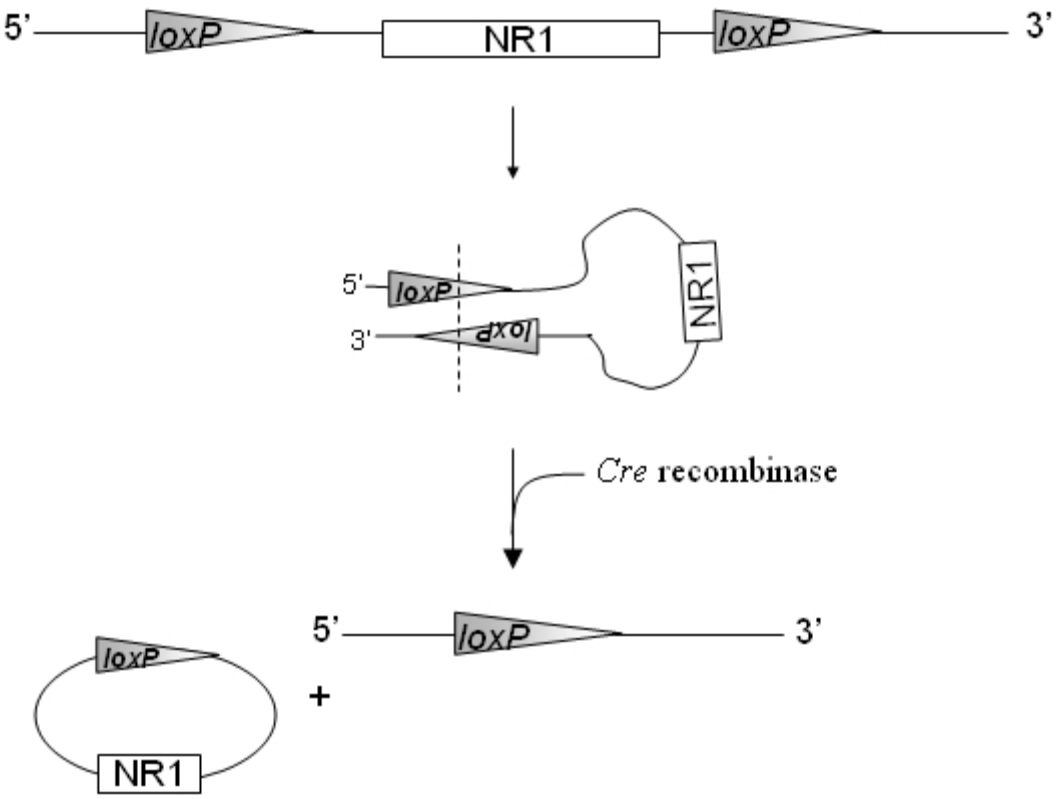

Figure 4-1: (**A**) Illustration of the *loxP* site. An 8 bp asymmetrical region is flanked by two palindromic regions. *Cre* recombinase cleaves in the assymetrical 8 bp region. (**B**) A schematic detailing *Cre-loxP* recombination. When the *loxP* sites are in a *cis* arrangement, they may be complimentarily cleaved by *Cre* recombinase (dashed line) and resealed to form two products. The circular DNA containing the gene of interest will be degraded naturally, and only a single *loxP* site remains on the chromosome.

Methods

NR1 Mutant Mice and HSA Transgenic line

Mice with a single floxed allele for the GRIN1 gene encoding the NR1 subunit of the NMDA receptor used in the experiments were initially created by Tsien *et al.* and purchased from Jackson Laboratories (Bar Harbor, Maine). This allele contains *loxP* sites flanking 9 exons of the Grin1 gene. (*loxP* inserts were placed between exons 10 and 11, and 3 kb downstream of the final exon) [**71**]. Human Skeletal Actin (HSA) transgenic mice were created by the Melki laboratory and have been repeatedly established to show skeletal muscle-specific expression of Cre recombinase [**40**]. These mice were received by our lab several years ago from Jackson Laboratories and have been breeding well. All animals are housed in a fully-equipped and staffed vivarium at The Ohio State University, under an IACUC approved protocol to Dr. Jill Rafael-Fortney, Department of Molecular and Cellular Biochemistry. Mice were housed on a standard 12 hr light/day cycle and were provided food (7012 Teklad LM-485 Mouse/Rat Sterilizable Diet, Harlan Laboratories) and water *ad libitum*.

NR1 flox (NR1) homozygous mice (NR1 flox/flox) were bred with mice carrying the HSA Cre transgene (Cre^+). The F1 generation resulted in NR1 heterozygous mice (NR1 flox/wt) with and without the transgene (Cre^+). Floxed heterozygotes containing the HSA Cre transgene (NR1 flox/wt Cre^+) were mated with the homozygous (NR1 flox/flox Cre^-) F1-generation mice to produce the F2 generation which contained the NR1 flox/flox Cre^+ (NR1 cKO). NR1 cKO mice from the F2 generation were utilized experimentally, with unfloxed and floxed Cre^- littermates being used as controls (see *Figure 4-2* in Results Section).

Genotyping of Mice

DNA from tail biopsies was analyzed by PCR. Primers utilized to screen for floxed-NR1 were used as described in Tsien *et al.* [**71**]. These included a forward primer for the flox allele, designed to detect a neomycin resistance gene inserted along with the *loxP* sites in creation of the mice, (5′ CTT GGG TGG AGA GGC TAT TC 3′) and a reverse primer (5′ AGG TGA GAT GAC AGG AGA TC 3′). For the wild-type (wt) allele, the forward primer was (5' GTG AGC TGC ACT TCC AGA AG 3') and the reverse primer was (5' GAC TTT CGG CAT GTG AAA TG 3'). Reactions for the flox and wild-type (wt) alleles were carried out on genomic DNA for 35 cycles under the following conditions: 94°C, 30 s; 61°C, 30 s; 72°C, 45 s. Primers utilized to screen for the HSA Cre trangene included forward primer (5′ AAG TGA AGC CTC GCT TCC 3′) and a reverse primer (5′ CCT CAT CAC TCG TTG CAT CGA 3′). Reactions were carried out on genomic DNA for 35 cycles under the following conditions: 94°C, 30 s; 55°C, 30 s; 72°C, 1 min. Following PCR, reaction products were run out on 1% agarose gels (Tris-boric acid-based buffer) containing ethidium bromide and photographed under UV light.

Histology

Tissues from mice sacrificed at 17 weeks were excised and embedded either unfixed (for epifluorescence) or fixed with formaldehyde (for confocal immunofluorescence; see protocol below) in a cryoprotective medium Tissue-Tek. Tissues were then frozen over isopentane in liquid nitrogen. Tissues were stored at -80ºC. Frozen sections (8 µm) of quadriceps, diaphragm and soleus were cut on a cryostat. Hematoxylin and eosin staining (H&E) was performed using standard procedure.

Immunofluorescence

For epifluorescence visualization, immunofluorescence for NR1 was conducted as previously described (*see Chapter* II) on 8 µm sections of unfixed frozen quadriceps with the primary polyclonal rabbit anti-NR1 antibody (Chemicon, 1:50 dilution) and secondary antibody CY3 α-rabbit (Jackson ImmunoResearch Laboratories**,** 1:200 dilution). NMJs were labeled with Alexa 488-conjugated α-bungarotoxin (1:1000) and all samples were counterstained with DAPI. Images were taken with a Nikon Eclipse 800 epifluorescence microscope using a SPOT-RT slider digital camera and Spot software.

For confocal microscopy, excised quadriceps were fixed in 1% *p*-formaldehyde (aq) for 1 hour and then stored in a sucrose solution (20% in KPBS) overnight. Tissues were embedded in Tissue-Tek and frozen over isopentane in liquid nitrogen. Immunofluorescence for NR1 was conducted as stated above on 8 µm sections. Images were taken with a Zeiss 510 META laser scanning microscope (Thornwood, New York) at 63x objective lens.

Immunoblots

Protein isolation, concentration measurement and western blotting was performed as previously described (*see Chapter* II) on total skeletal muscle isolated from NR1 conditional mice at 17 weeks of age; *mdx* (dystrophin knockout) and *dko* (utrophin and dystrophin knockout) at 10 weeks of age. Both an NR1 antibody specific to the C-terminus (Chemicon, 1:500 dilution) and specific to the "pan region" (Pharmingen, 1:250) were used. Brain taken from C57 Bl/10 mice were used as positive controls.

Results

Generation of NR1 loxP-Cre mice.

Figure 4-2

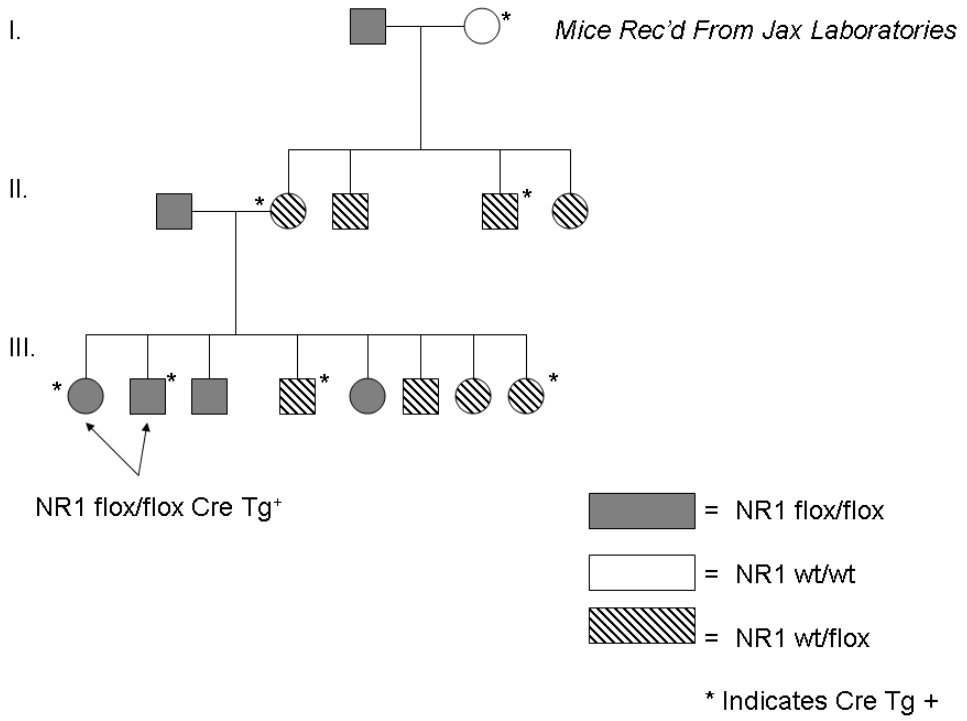

Figure 4-2: Mating pedigree for NR1 cKO mice. (I) NR1 flox/flox Cre Tg^- x NR1 wt/wt Cre Tg^+ yielded NR1 flox/wt Cre $Tg^{-/+}$ litters. (II) A heterozygote (NR1 flox/wt Cre Tg^+) was mated with a homozygote (NR1 flox/flox Cre Tg^-) to yield a variety of offspring (III) of which approximately 25% were the correct genotype of interest, NR1 flox/flox Cre Tg^+.

NR1 flox/flox Cre^- mice were bred with mice carrying the NR1 wt/wt Cre^+. PCR was used to determine genotypes of offspring (*Figure 4-3*). The F1 generation consisted of NR1 heterozygous mice (NR1 flox/wt) with and without the *Cre* transgene (Cre^+). Heterozygous Cre^+ mice (NR1 flox/wt Cre^+) were then mated to the homozygous mice (NR1 flox/flox Cre^-) to produce the F2 generation, containing all expected genotypes in Mendelian ratios (10:15:21:13) for heterozygous transgenic positive (NR1 flox/wt Cre^+), heterozygous transgenic negative (NR1 flox/wt Cre^-), homozygous transgenic negative

(NR1 flox/flox Cre$^-$) and NR1 cKO (NR1 flox/flox Cre$^+$), respectively. NR1 cKO mice from the F2 generation were used experimentally (*Figure 4-2*). All phenotypes of mice appeared overtly normal up to 12 months of age.

In later experiments, NR1 cKOs were mated with each other to create "double-transgenic" mice. Though PCR could not used to identify double-transgenics, as the transgene band was already strong in PCR (see *Figure 4-3*), we decided to analyze all mice histologically and later confirm genotypes if advantageous or necessary.

Figure 4-3

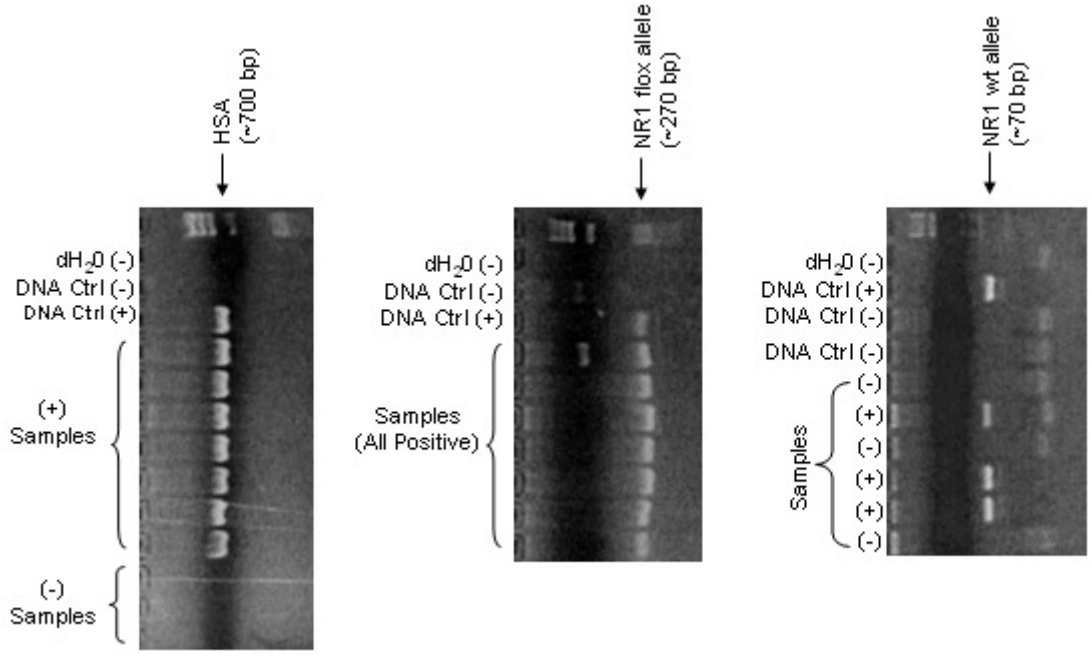

Figure 4-3: PCR products of mouse genotyping (representative samples) separated on 1% agarose gels containing ethidium bromide. Wild-type (wt) product is expected at ~70 bp, flox product at ~270 bp, and transgene product at ~700 bp. * On rare occasion, the neo resistance cassette (detects *Cre* transgene on PCR) can be amplified dependent upon number of copies of the cassette present.

Muscle Damage is not apparent at 17 weeks of age in NR1 KO mice.

In humans and mice with muscular dystrophy, extensive skeletal muscle damage is present. Therefore, we first investigated whether NR1 cKO mice displayed a similar phenotype. Muscle damage is characterized by a severe atrophy or loss of muscle fibers, the appearance of regenerating fibers as signaled by centrally-localized nuclei and/or the

presence of inflammation. However, *Figure 4-4* shows that no extensive muscle damage was observed in the NR1 cKO mice—they were histologically comparable with control mice. All mice had similar-sized muscle fibers, with nuclei located peripherally denoting non-regenerating fibers and no inflammation. These data suggested one of three scenarios: (1) *Cre* was not functioning to excise this particular *loxP* flanked gene; (2) *Cre* was not expressed in synaptic nuclei of the NMJ where NR1 is exclusively expressed (*Figure 2-2*); or (3) NR1 is being excised, but the mice do not show muscle-degeneration phenotype, unsupportive of our hypothesis.

Figure 4-4

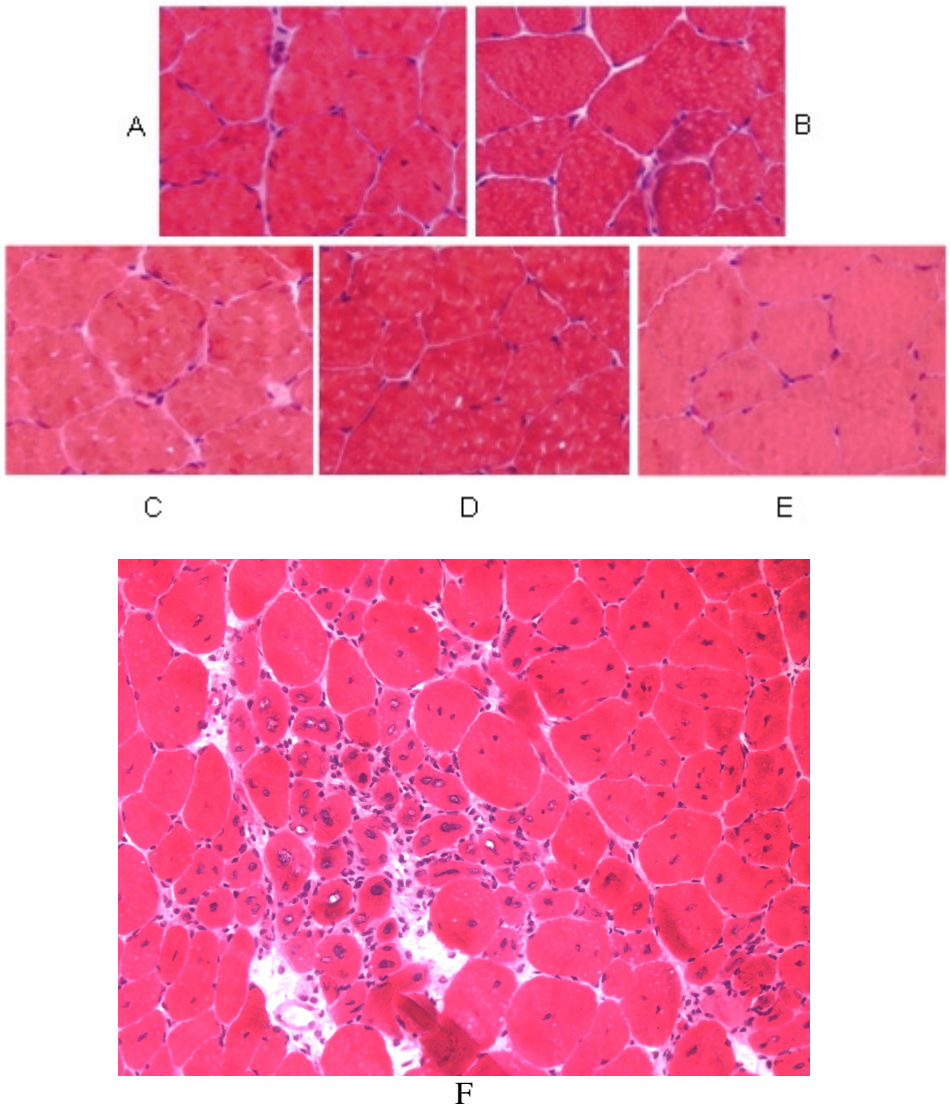

Figure 4-4: H&E staining of mice quadriceps at 17 weeks of age. Genotypes represented are: NR1 flox/flox Cre^{+} **(A & B)**, NR1 flox/wt Cre^{+} **(C)**, NR1 flox/flox Cre^{-} **(D)** and NR1 wt/wt Cre^{+} **(E)**. For comparison, muscle degeneration is seen in a severe muscular dystrophy mouse model [*dko*] **(F)**. An occasional fiber with central nuclei was observed **(A)**, but not statistically different between genotypes. All images at 40X magnification, except *dko* shown at 20X. *dko slide courtesy of K. Gardner, Rafael-Fortney Laboratory.*

Localization of NR1 in cKO and control skeletal muscle.

Following our negative histology data, we decided to confirm deletion of NR1 protein from skeletal muscle via immunfluorescence in NR1 cKO mice. *Figure 4-5* shows NR1-staining of skeletal muscle in mice aged 17 weeks. Staining revealed no remarkable distinction between NR1 cKOs and control littermates, in that NR1 staining

was present in all genotypes. We tested a number of antibodies commercially available for NR1 to try and identify one that was truly specific for NR1 and was also sensitive enough to detect the very small amount of NR1 in skeletal muscle (over 90% of skeletal muscle proteins are from the contractile apparatus). We used western blot analysis to examine differences in NR1 protein levels and confirm antibody specificity (*Figure 4-6*). Interestingly, two bands were observed on western analysis; one smaller and one larger than the molecular weight of the positive control band (murine brain). The antibody used (mouse monoclonal NR1 anti-rabbit from Chemicon) is specific for the C-terminus of the NR1 protein. Incidentally, a second antibody (mouse monoclonal NR1 anti-rabbit from Pharmingen), which is specific to the NR1 "pan region" (*see Chapter* II), yielded similar results (*Figure 4-7*). Additionally, *dko*, *mdx* and C57 muscle samples were analyzed for comparison (*Figure 4-7*). The *dko* and *mdx* are mouse models of muscular dystrophy (severe and mild, respectively). The C57 Bl/10 mouse is a phenotypically normal mouse. All samples contain the double-banding pattern except the *mdx* sample, which appears to have a single band.

Figure 4-5

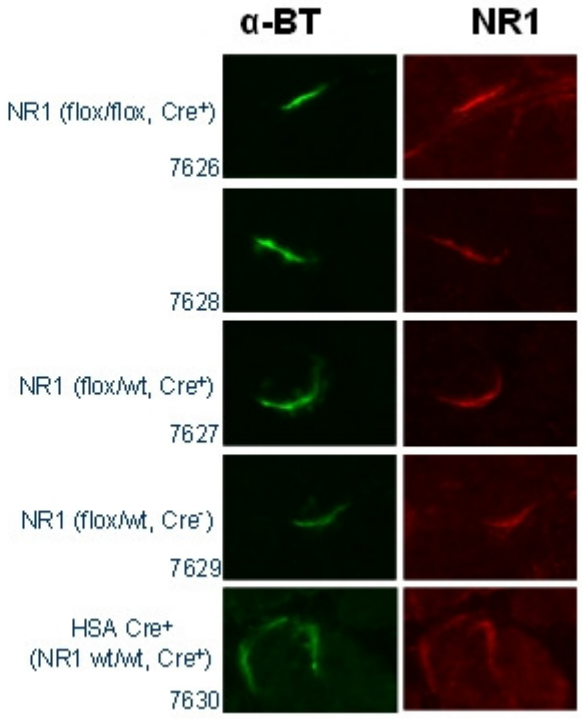

Figure 4-5: Immunofluorescence analysis of the NMJ. Green immunofluorescence indicates α-BT staining of Ach receptors, with red indicating presence of NR1 (NR1). Overlap is indicative of NR1 localizing at the NMJ, and is evident in all samples, including NR1 KO tissues. (Representative samples are shown). Numbers refer to individual mice.

Figure 4-6

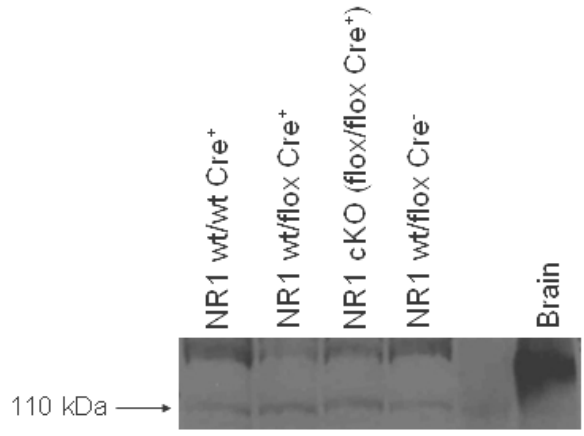

Figure 4-6: Western Blot analysis of the NR1 protein. NR1 C-terminus monoclonal antibody (Chemicon, 1:500 dilution) was used to detect levels of NR1 protein. All samples yielded two bands; one at ~110 kDa and one slightly larger than 120 kDa. Brain was utilized as a positive control. (Representative samples are shown).
.

Figure 4-7

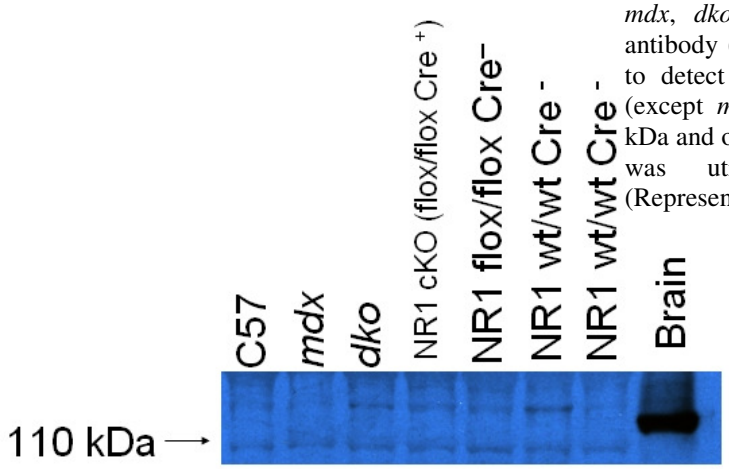

Figure 4-7: Western Blot analysis of the NR1 protein "pan region" on NR1 flox genotypes, *mdx*, *dko*, and C57 Bl/10. NR1 monoclonal antibody (Pharmingen, 1:250 dilution) was used to detect levels of NR1 protein. All samples (except *mdx*) yielded two bands; one at ~110 kDa and one slightly greater than 120 kDa. Brain was utilized as a positive control. (Representative samples are shown).

After determining that NR1 was not knocked out at the NMJ, we examined the immunofluorescently stained sections (*Figure 4-5*) further via confocal microscopy. The aim was to determine whether NR1 was simply not being targeted at the NMJ: was NR1 still expressed in synaptic nuclei, was it expressed by the neuron, or was our *Cre* working properly and immunofluorescence showed NR1 expression at the NMJ pre-synaptically but not at post-skeletal muscle membrane? Determining the localization of NR1 with more detail than what epifluorescence could show would answer these questions and redirect further investigation. *Figure 4-8* illustrates that the NMJs of NR1 cKO mice and wild-type mice each had identical localization patterns, confirming that our *Cre* was ineffective at ablating NR1 in synaptic nuclei.

Figure 4-8

A.

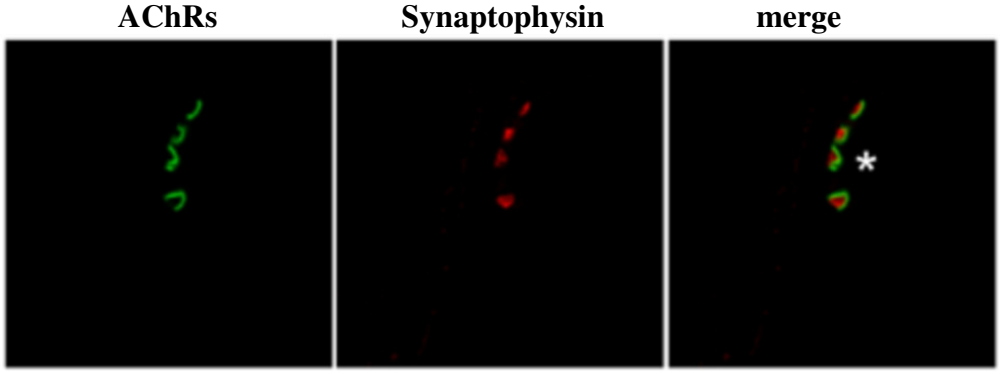

B.

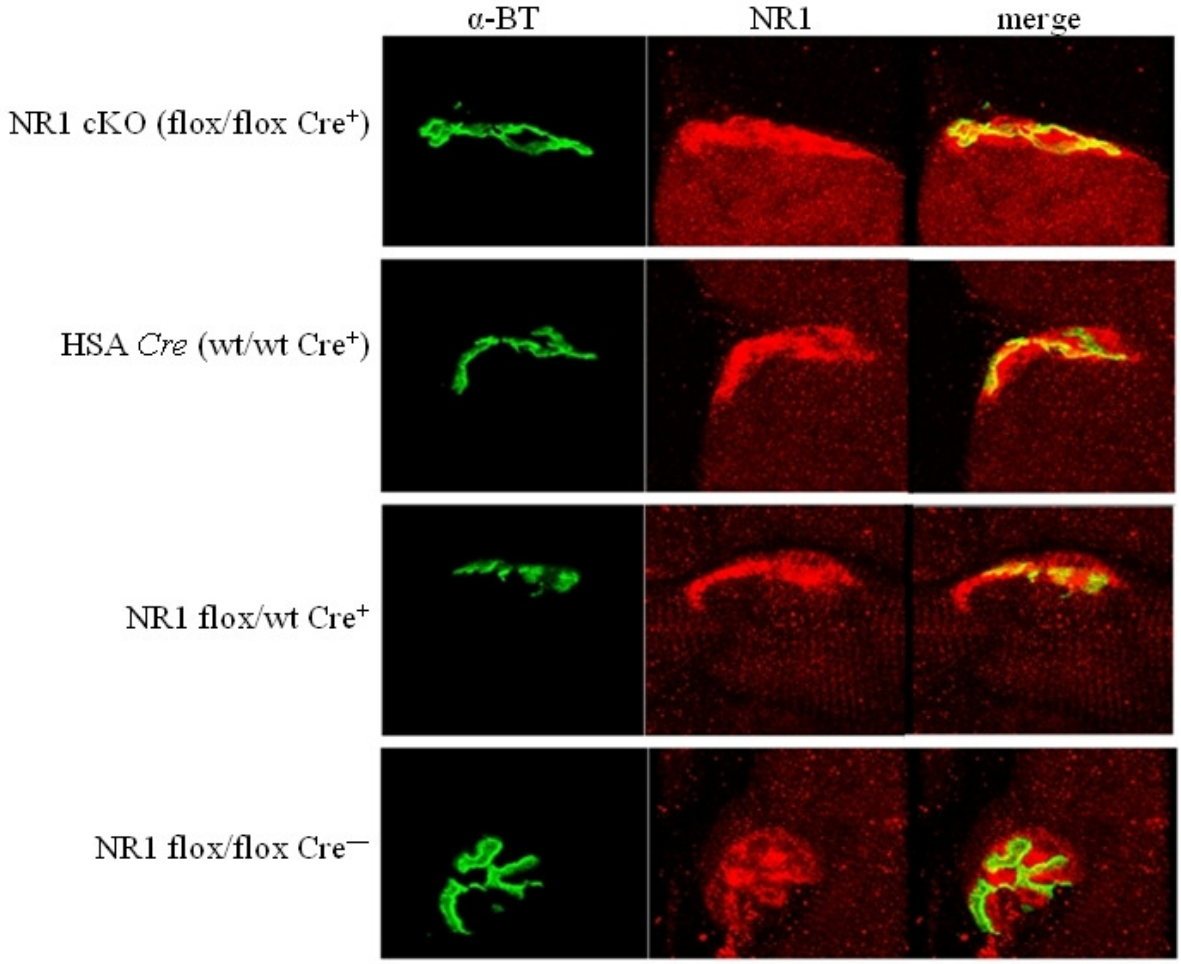

Figure 4-8: (**A**) Epifluorescence of the NMJ with synaptophisin, a pre-synaptic protein, illustrating that pre- and post-synaptic membranes can be differentiated using immunofluorescence. Asterisk (*) indicates post-synaptic side of the junction. *Image courtesy of Mays et al.* [**38**]. (**B**) Confocal microscopy using Alexa 488-conjugated α-Bungarotoxin (first column) to identify ACh receptors at the primary folds of the NMJ and CY3-conjugated NR1 anti-rabbit (polyclonal, Chemicon, middle column) detection to mark NR1 subunits. NR1 localizes to the NMJ in all genotypes of mice. Representative NMJs shown. (63X objective lens used, 3x zoom).

Discussion

In this study, we attempted to test the hypothesis that absence of NR1 from the murine NMJ will result in abnormal skeletal muscle maintenance and development. However, our efforts to knockout the NR1 gene from skeletal muscle and therefore eliminate the expression of a functional NMDA receptor at the NMJ were unsuccessful as shown by immunofluorescence and western analysis using NR1-spcific antibodies. Confocal microscopy revealed that NR1 subunits continued to localize to the NMJ post-synaptic membrane in NR1 cKOs (*Figure 4-8*). Therefore the stated hypothesis could not be tested due the *Cre-loxP* gene excision strategy not functioning properly.

Although the HSA *Cre* mouse line was designed to be expressed in skeletal muscle during development and differentiation, it was designed neither to be specific for nor inclusive of synaptic nuclei [**4**]. Like ACh receptor subunits, NR1 may be expressed exclusively from synaptic nuclei. Utilizing a *Cre* coupled with a different gene promoter might provide a more ideal recombination system for NR1 at the NMJ. For example, coupling the *Cre* transgene to a synaptic nucleus-specific gene promoter would allow *Cre* expression exclusively to that locus. Currently, the *Cre* transgene has not been coupled with any such gene promoters, however, plausible candidate genes include ACh receptors [**39**], neuregulin receptors (erbB2 and erbB4 components) [**65**] S-laminin or a membrane-associated cell adhesion molecule N-CAM [**41**].

The age of mice at sacrifice must also be considered. In this thesis, we show data in which mice were aged to 17 weeks before sacrifice; however we later conducted the same immunofluorescence experiments in cKO mice at ages 8, 10, 12 and 52 weeks. These mice expressed the same phenotypes as the 17-week aged mice (data not shown).

The 17-week old mice were chosen to represent all data, as by that point, ample time was assumed for complete *Cre* recombinase expression and formation, and protein turnover to have occurred.

A caveat to this, however, is that we did not check *Cre* expression in the mice or confirm synaptic nuclei-specific expression of the NR1 gene, which would have required time-consuming and labor-intensive RNA *in situ* experiments. To confirm *Cre* gene expression, Tsien *et al.* utilized a highly-specific antibody against *Cre* recombinase and showed localization exclusively to the area of interest (CA-1 region of the hippocampus). We suspect that *Cre* was expressed in muscle fibers where NR1 is not shown to be expressed, thus no phenotype would be observed. To test this hypothesis, we can use an anti-*Cre* antibody to investigate localization via immunofluorescence, or can test for the presence of *Cre* recombinase via western blot analysis. It is likely that synaptic nuclei do not express the gene promoter (α-actin) to which *Cre* was coupled in our construct. We would therefore expect *Cre* to be found as localized to the body of the muscle fiber rather than the synapse.

Of particular note, our western blot analysis shows two NR1 bands using the "pan region" antibody and two bands using the C-terminus polyclonal antibody. The sizes of the bands at 110-120 kDa, are consistent with literature values reported in brain (due to alternative splicing, protein size varies; *see Chapter* II) [**31, 69**]. We must, however, acknowledge the possibility that the NR1 antibodies utilized may not be specific to the NR1 protein isoforms. Homologous proteins, with only a few amino acids varying from the epitopes which anti-NR1 antibodies detect, are certainly possible in skeletal muscle. But, the difference in size of NR1 isoforms shown is consistent with data previously

generated (*see Chapter* II) reinforcing the suggestion of alternative splicing in the NR1 gene in skeletal muscle.

While the NR1 cKO mice did not work as predicted in these experiments, we did observe two bands in western blot analysis using two different NR1 antibodies. Further experiments could determine if *Cre* is expressed at the NMJ under the HSA promoter, or perhaps a different *Cre* system might be specifically knocked-out in the NR1 gene.

V.

Discussion and Future Directions

Localization of the NR1 subunit

The studies I present in this thesis sought to test the overarching hypothesis that NR1, the functional and obligatory subunit of NMDA receptors, functions in the development and maintenance of skeletal muscle fibers. We first used immunofluorescence to show that NR1 localizes between one and seven days post-birth, coinciding with fiber-type differentiation. Though it can not be definitively stated that functional NMDA receptors are formed at that junction in the same timeframe, demonstrating a chronologic correlation of the functionally obligatory subunit with fiber-type differentiation supports the hypothesis that NMDA receptors are involved in fiber-type determination. As NR1 must complex with NR2x subunits to create a functional receptor, the evidence presented here warrants further investigation as to the localization timeframe of other glutamate receptor subunits, including NR2A and NR2B. Should the timeframe correspond to NR1 localization, it might be beneficial to use co-immunoprecipitation to isolate the protein complex formed to create the functional receptors. Identification of the components of functional NMDA receptors in muscle will further delineate the functional roles of the receptors and will provide insight into the modulation of these receptors for therapeutic purposes. In the brain, identification of the NMDA complex components has led to therapeutics specifically targeted to affect binding and activity of the channels to which they are linked [**52**].

Whether NMDA receptor localization is disrupted in murine models of muscular dystrophy has not yet been published. In dystrophin/utrophin double-knockout (dko)

mice, slow muscle fiber-types are predominant in limb muscles where mixed fiber-types are typical in normal mice [**2**]. If irregular or disrupted localization of NMDA receptors in skeletal muscle could be correlated to fiber-type differentiation in *dko* mice, stronger evidence of a functional role would be present. Data recently generated in our laboratory show disrupted localization of both AMPA and NMDA receptors in *mdx* and *dko* mouse models at 10 weeks of age [data not shown]. However, NR1 protein expression levels would represent a better comparison between these models, but the western blot analysis requisite for comparing protein levels is dependent upon finding a functional primary anti-NR1 antibody (*Chapter* II). Despite this setback, further analysis of glutamate receptor complexes in *dko* skeletal muscle might provide useful insight into the workings of the NMJ and warrants further investigation.

Primary Structure of the NR1 subunit

As structure often directly correlates with function, investigation of the primary structure of NR1 found in skeletal muscle might allude to its function there. To determine the protein structure of NR1 expressed in skeletal muscle, we amplified NR1 mRNAs from skeletal muscle. Using reverse transcriptase, we created the corresponding cDNA sequence, which was then compared to known splice variants found in brain, as NR1 is known to be alternatively spliced at no less than three exons [**46, 78**]. While RT-PCR was able to amplify two bands in skeletal muscle, the NR1 complex transcripts have not yet led to definite sequences. Instead, what is believed to be a complex mixture of two sequences was isolated from a lower band and the upper band was inconclusive.

If there are in fact multiple sequences being expressed, inserting each sequence into separate plasmids might allow for the sequences to be identified. Bacterial plasmids

digested with restriction enzymes using a ligation reaction. Each plasmid would theoretically only incorporate one of the sequences. Plasmids could then be transformed into competent *E. coli* cells, plated and the correct plasmid incorporation could be confirmed via PCR. Transformed *E. coli* can be cultured to create clonal colonies, from which plasmid DNA can be isolated for sequencing.

Another way we could approach determination of primary amino acid structure would be to directly test the protein variants. Using an SDS-PAGE gel, we could isolate proteins via molecular weight (and, if necessary, by charge). The proteins of interest could be identified by staining, excised from the gel; then digested with a protease (e.g. chymotrypsin). The resultant protein fragment mixture could be analyzed by mass spectroscopy and computationally compared to known amino acid sequences in a database to identify likely candidates for the protein's identity. Due to the protein's size, Edmund degradation (identification of individual amino acids sequentially via biochemical analysis) is unlikely to be successful. Unlike RT-PCR analysis, this method would identify post-translational alterations to the protein isoforms identified. Enzymatic activity with NR1 at the NMJ, miRNA interference or protein modification studies are all potential avenues for further research, dependent upon the outcome of the NR1 sequencing studies. Correlation of any of these with skeletal muscle pathology offers the possibility of novel therapeutics and treatments.

Physiological Role of Glutamate Receptors in Skeletal Muscle

A third goal of these studies was to determine functionality of NMDA receptors in skeletal muscle. Two methods were used to test functionality. First, we measured the effects of blocking the entire glutamatergic system in skeletal muscle and blocking

AMPA and NMDA receptors at this system. Using electrophysiology we observed that shutting down the glutamate system increases mEPP frequency and quantal content. In other words, there is an increase in vesicle release between axonal firing, suggesting instability in the neuronal firing mechanisms. Presumably, the next step would be to repeat the experiment in *mdx* mice, to determine whether this system functions differently in a disease model. In this experiment, we would first establish a baseline of the difference in mEPP frequency and quantal content between the untreated control *mdx* myocytes. We would then observe changes in *mdx* myocytes after treatment with glutamate agonists and antagonists.

Our second experiment was to excise expression of NR1 exclusively in skeletal muscle to disrupt NMDA receptor function. However, our hypothesis for that experiment was unable to be tested, as confocal microscopy revealed that our *Cre-loxP* system was not functioning as expected. In addition to the alternatives listed in *Chapter* IV, another potential idea would be to deliver adeno-associated virus (AAV) expressing *Cre* recombinase to skeletal muscle. This technique might allow for *Cre* to be expressed at high enough levels to excise floxed NR1 from synaptic nuclei. If, via a *Cre* induced mechanism or other means, we were able to ablate or disrupt receptors exclusively from skeletal muscle, the next step could be to generate a rescue model for any phenotypes observed due to NR1 cKO.

The purpose of excising the NR1 gene was to eliminate the NR1 protein. We have not yet correlated protein expression levels with disease; as stated above, a great barrier to determining protein expression levels has been finding a functional antibody for NR1. However, we might be able to decrease protein expression levels by using RNA

interference (RNAi) to down-regulate expression of NR1. In C57 BL/10 mice, knocking down the expression of the NR1 gene via micro-RNA (miRNA) or small interfering RNA (siRNA) could lead to demonstration of synaptic cells' dependency on these receptors for normal function. That is to say, we might induce a phenotypical change in normal mice by impeding transcription or translation of the NR1 subunit. The caveat to this, unfortunately, is that without a working NR1 antibody, quantifying protein levels for confirmation of the system is still troublesome.

Glutamate toxicity, the "over-loading" of a synapse due to excess glutamate neurotransmitter, is another possibility which might be investigated in skeletal muscle. As the neuron is overwhelmed with glutamate, it becomes less sensitive to action potentials and eventually dies. Huntington's disease, amyotrophic lateral sclerosis and several other neurodegenerative disorders display glutamate toxicity as a contributing to or resulting from pathogenesis [**9**]. An investigation into the localization of glutamate neurotransmitter in skeletal muscle recently showed severe disruption of glutamate in skeletal muscle. Localization exclusive to the NMJ in normal mice is rendered to uncontained, ubiquitous extracellular localization in severe models of mouse muscular dystrophy [Rafael-Fortney laboratory, unpublished]. Though the possibility exists that pathology causes this disruption as a phenotype, our physiology data of NMDA receptors in skeletal muscle suggest that the gluatamatergic system plays a role in normal NMJ functionality.

It would be worthwhile to quantify glutamate levels in skeletal muscle for comparison between normal and diseased state. Using ^{1}H- and ^{13}C-labeling and nuclear magnetic resonance (NMR), researchers have quantified glutamate levels in brain and

using heart respectively [**58, 74**]. Additionally, chromatography techniques (gas, HPLC) or enzymatic assays might be potential venues to determine glutamate levels.

Limitations

There are two major limitations two the findings presented in this thesis. First, antibody specificity is still inconclusive. We tested numerous commercially-available NR1 antibodies in western blots and immunofluorescence, but the results were often inconclusive and somewhat contradicting. However, we propose that this is due to alternative splicing of the NR1 gene in skeletal muscle that is not consistently detected by antibodies we tested. The greatest challenge remains in finding (or perhaps designing) an antibody which can clearly and consistently detect the NR1 isoforms that we believe it exist at the NMJ.

Second, as mentioned in *Chapter* III, our physiology experiments were not statistically significant after a paired two-tailed *t*-test, due primarily to sample size. However, a definite trend of both increased mEPP frequency and quantal content could be observed after blocking the entire glutamate system. Given the dramatic difference seen between samples in the physiology traces, coupled with p values of nearly ≤ 0.05, we believe that increasing the sample size of semitendonosus muscles examined will show a significant difference between control and treated samples. For all mouse studies not involved with electrophysiology, generally >5 mice were tested in each experiment.

Conclusion

Taken together, the data presented in this thesis provide credible evidence that the NR1 subunit is present and functional at the NMJ in murine skeletal muscle. The presence of NR1 has been demonstrated via immunofluorescence and western blotting,

its expression determined via RT-PCR, and its functionality tested physiologically via single-cell electrophysiology studies with glutamate receptor agonists and antagonists. The presence of both NMDA receptors and AMPA receptors [**38**] is important in that it challenges a long-held dogma that the NMJ functions as a "simple cholinergic synapse." An alternative glutamatergic system opens the door for novel therapeutics and treatments which might correlate with disease state of the NMJ. Insight into the workings of the NMJ can be revealed upon further investigation of this novel glutamatergic system.

Appendix A

Key: **Grin1/NR1** — Known sequence of NR1; **4_1_No_He**—isolated sequence from skeletal muscle.

```
Grin1/NR1   ACCCATGTCA TCCCAAATGA CAGGAAGATC ATCTGGCCAG GAGGAGAGAC AGAGAAGCCT
            TGGGTACAGT AGGGTTTACT GTCCTTCTAG TAGACCGGTC CTCCTCTCTG TCTCTTCGGA
            __________a__________a__________a__________a__________a__________>

1. 4_1_No_He                                      10         20         30
[  564 ]                                 ANATN GCNAGANCNN AAAGACCCCN TTAAAAG-GG>
                                         | ||      |  |    | ||        | |||
Grin1/NR1                                AGATC ATCTGGCCAG GAGGAGAGAC AGAGAAGCCT
```

```
                                                  1300
Grin1/NR1   CGAGGATACC AGATGTCCAC CAGACTAAAG ATAGTGACAA TCCACCAAGA ACCCTTCGTG
            GCTCCTATGG TCTACAGGTG GTCTGATTTC TATCACTGTT AGGTGGTTCT TGGGAAGCAC
            __________a__________a__________a__________a__________a__________>

1. 4_1_No_He    40          50         60             70         80         90
[  564 ]    CAAAAAAAGC ACCT-TCAGC NNGNCNNAGG A-A-TG-GGC TTCTNCANCN TTTTNGGGNT>
            | |  | | | |  | ||  |   | |  | | | | ||     | |  ||           |
Grin1/NR1   CGAGGATACC AGATGTCCAC CAGACTAAAG ATAGTGACAA TCCACCAAGA ACCCTTCGTG
```

```
Grin1/NR1   TATGTCAAGC CCACAATGAG TGATGGCACA TGCAAAGAGG AGTTCACAGT CAATGGTGAC
            ATACAGTTCG GGTGTTACTC ACTACCGTGT ACGTTTCTCC TCAAGTGTCA GTTACCACTG
            __________a__________a__________a__________a__________a__________>

1. 4_1_No_He       100        110           120         130        140
[  564 ]    CNTGGTNTGN NTTTTTTGAN T--TGGTGTN TTTTTTTTGG -GCTCTGNAT CTNT-TTANT>
              ||    |        |||  |  |||     |       ||  | ||    | |  |  |
Grin1/NR1   TATGTCAAGC CCACAATGAG TGATGGCACA TGCAAAGAGG AGTTCACAGT CAATGGTGAC
```

```
                         1400
Grin1/NR1   CCTGTCAAGA AGGTGATCTG TACGGGGCCT AATGACACAT CCCCAGGAAG CCCACGTCAC
            GGACAGTTCT TCCACTAGAC ATGCCCCGGA TTACTGTGTA GGGGTCCTTC GGGTGCAGTG
            __________a__________a__________a__________a__________a__________>

1. 4_1_No_He 150         160        170         180        190        200
[  564 ]    TATNAC-TTA TATTGATTTN TNNNNNTTGG TAT-ACTCAN CATNTCNAAN GTGGANTAAT>
              |  |   |    |||| |  |           || || ||  |      ||        | |
Grin1/NR1   CCTGTCAAGA AGGTGATCTG TACGGGGCCT AATGACACAT CCCCAGGAAG CCCACGTCAC
```

```
                                                                        1500
Grin1/NR1   ACAGTGCCCC AGTGCTGTTA TGGCTTCTGC GTTGACCTGC TCATCAAGCT GGCACGGACC
            TGTCACGGGG TCACGACAAT ACCGAAGACG CAACTGGACG AGTAGTTCGA CCGTGCCTGG
            __________a__________a__________a__________a__________a__________>
```

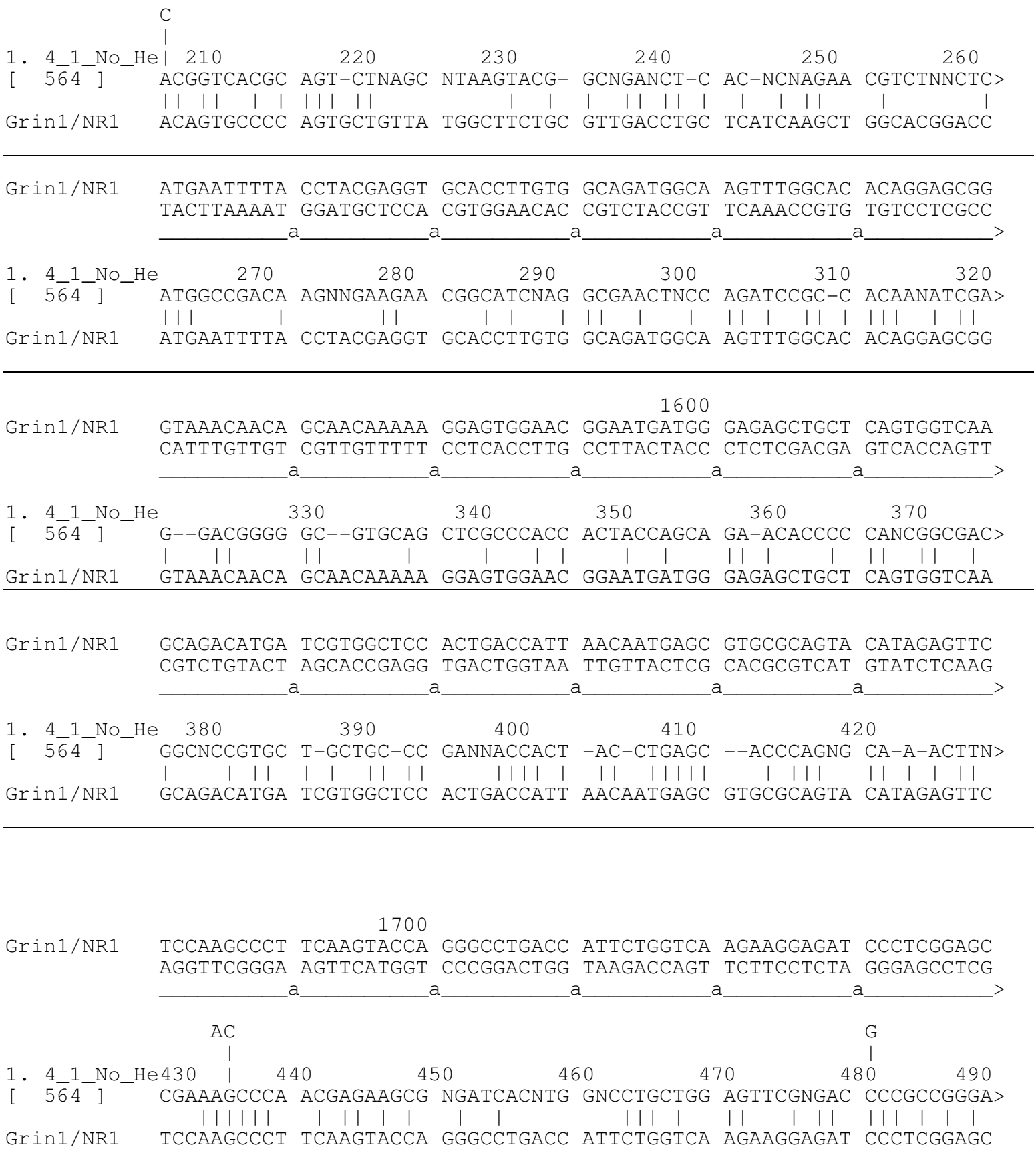
C
1. 4_1_No_He 210 220 230 240 250 260
[564] ACGGTCACGC AGT-CTNAGC NTAAGTACG- GCNGANCT-C AC-NCNAGAA CGTCTNNCTC>
Grin1/NR1 ACAGTGCCCC AGTGCTGTTA TGGCTTCTGC GTTGACCTGC TCATCAAGCT GGCACGGACC
Grin1/NR1 ATGAATTTTA CCTACGAGGT GCACCTTGTG GCAGATGGCA AGTTTGGCAC ACAGGAGCGG
TACTTAAAAT GGATGCTCCA CGTGGAACAC CGTCTACCGT TCAAACCGTG TGTCCTCGCC
1. 4_1_No_He 270 280 290 300 310 320
[564] ATGGCCGACA AGNNGAAGAA CGGCATCNAG GCGAACTNCC AGATCCGC-C ACAANATCGA>
Grin1/NR1 ATGAATTTTA CCTACGAGGT GCACCTTGTG GCAGATGGCA AGTTTGGCAC ACAGGAGCGG
1600
Grin1/NR1 GTAAACAACA GCAACAAAAA GGAGTGGAAC GGAATGATGG GAGAGCTGCT CAGTGGTCAA
CATTTGTTGT CGTTGTTTTT CCTCACCTTG CCTTACTACC CTCTCGACGA GTCACCAGTT
1. 4_1_No_He 330 340 350 360 370
[564] G--GACGGGG GC--GTGCAG CTCGCCCACC ACTACCAGCA GA-ACACCCC CANCGGCGAC>
Grin1/NR1 GTAAACAACA GCAACAAAAA GGAGTGGAAC GGAATGATGG GAGAGCTGCT CAGTGGTCAA
Grin1/NR1 GCAGACATGA TCGTGGCTCC ACTGACCATT AACAATGAGC GTGCGCAGTA CATAGAGTTC
CGTCTGTACT AGCACCGAGG TGACTGGTAA TTGTTACTCG CACGCGTCAT GTATCTCAAG
1. 4_1_No_He 380 390 400 410 420
[564] GGCNCCGTGC T-GCTGC-CC GANNACCACT -AC-CTGAGC --ACCCAGNG CA-A-ACTTN>
Grin1/NR1 GCAGACATGA TCGTGGCTCC ACTGACCATT AACAATGAGC GTGCGCAGTA CATAGAGTTC
1700
Grin1/NR1 TCCAAGCCCT TCAAGTACCA GGGCCTGACC ATTCTGGTCA AGAAGGAGAT CCCTCGGAGC
AGGTTCGGGA AGTTCATGGT CCCGGACTGG TAAGACCAGT TCTTCCTCTA GGGAGCCTCG
AC
G
1. 4_1_No_He 430 440 450 460 470 480 490
[564] CGAAAGCCCA ACGAGAAGCG NGATCACNTG GNCCTGCTGG AGTTCGNGAC CCCGCCGGGA>
Grin1/NR1 TCCAAGCCCT TCAAGTACCA GGGCCTGACC ATTCTGGTCA AGAAGGAGAT CCCTCGGAGC

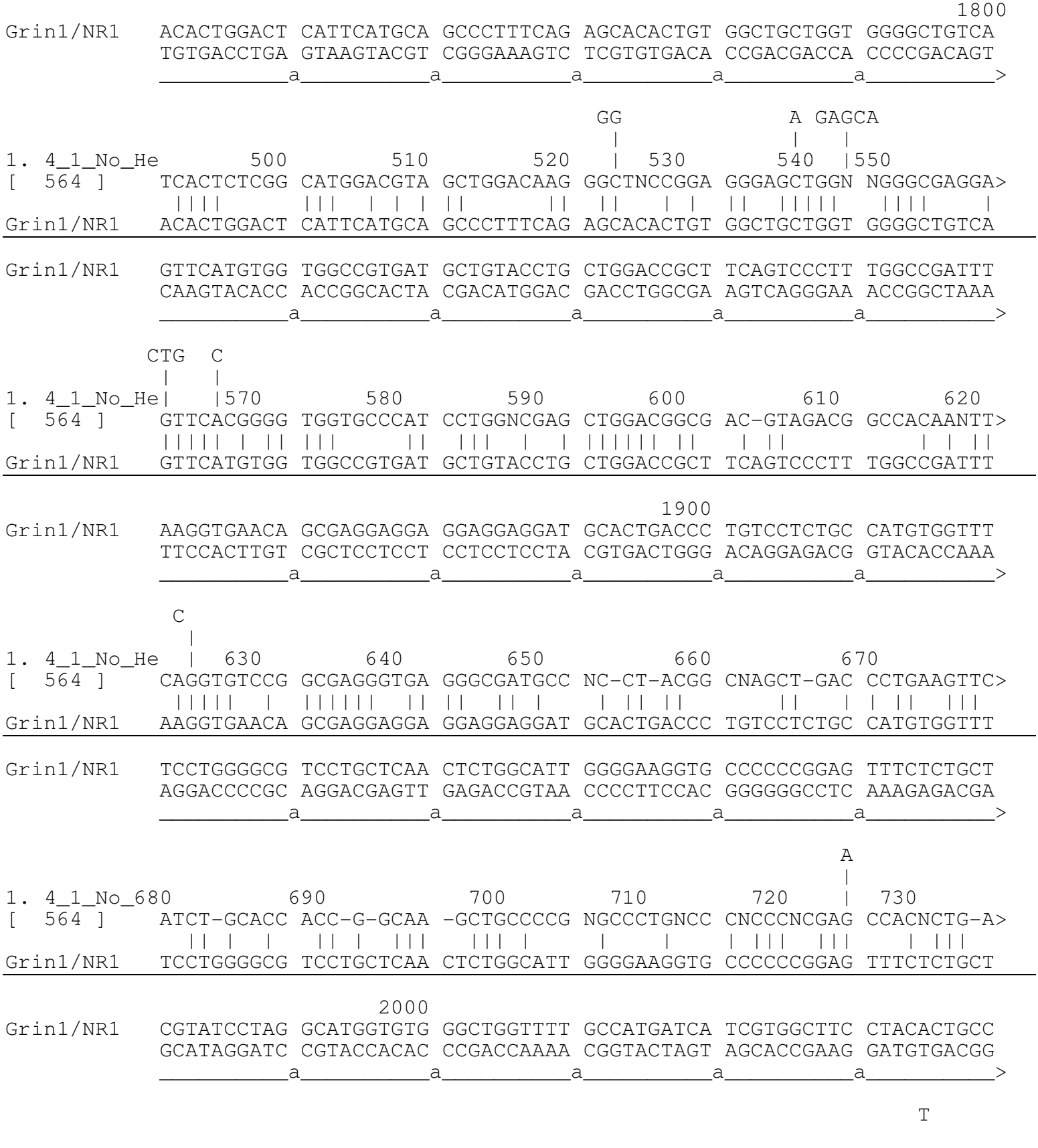
1800
Grin1/NR1 ACACTGGACT CATTCATGCA GCCCTTTCAG AGCACACTGT GGCTGCTGGT GGGGCTGTCA
TGTGACCTGA GTAAGTACGT CGGGAAAGTC TCGTGTGACA CCGACGACCA CCCCGACAGT
GG
A GAGCA
1. 4_1_No_He 500 510 520 530 540 550
[564] TCACTCTCGG CATGGACGTA GCTGGACAAG GGCTNCCGGA GGGAGCTGGN NGGGCGAGGA
Grin1/NR1 ACACTGGACT CATTCATGCA GCCCTTTCAG AGCACACTGT GGCTGCTGGT GGGGCTGTCA
Grin1/NR1 GTTCATGTGG TGGCCGTGAT GCTGTACCTG CTGGACCGCT TCAGTCCCTT TGGCCGATTT
CAAGTACACC ACCGGCACTA CGACATGGAC GACCTGGCGA AGTCAGGGAA ACCGGCTAAA
CTG C
1. 4_1_No_He 570 580 590 600 610 620
[564] GTTCACGGGG TGGTGCCCAT CCTGGNCGAG CTGGACGGCG AC-GTAGACG GCCACAANTT
Grin1/NR1 GTTCATGTGG TGGCCGTGAT GCTGTACCTG CTGGACCGCT TCAGTCCCTT TGGCCGATTT
1900
Grin1/NR1 AAGGTGAACA GCGAGGAGGA GGAGGAGGAT GCACTGACCC TGTCCTCTGC CATGTGGTTT
TTCCACTTGT CGCTCCTCCT CCTCCTCCTA CGTGACTGGG ACAGGAGACG GTACACCAAA
C
1. 4_1_No_He 630 640 650 660 670
[564] CAGGTGTCCG GCGAGGGTGA GGGCGATGCC NC-CT-ACGG CNAGCT-GAC CCTGAAGTTC
Grin1/NR1 AAGGTGAACA GCGAGGAGGA GGAGGAGGAT GCACTGACCC TGTCCTCTGC CATGTGGTTT
Grin1/NR1 TCCTGGGGCG TCCTGCTCAA CTCTGGCATT GGGGAAGGTG CCCCCCGGAG TTTCTCTGCT
AGGACCCCGC AGGACGAGTT GAGACCGTAA CCCCTTCCAC GGGGGGCCTC AAAGAGACGA
A
1. 4_1_No_680 690 700 710 720 730
[564] ATCT-GCACC ACC-G-GCAA -GCTGCCCCG NGCCCTGNCC CNCCCNCGAG CCACNCTG-A
Grin1/NR1 TCCTGGGGCG TCCTGCTCAA CTCTGGCATT GGGGAAGGTG CCCCCCGGAG TTTCTCTGCT
2000
Grin1/NR1 CGTATCCTAG GCATGGTGTG GGCTGGTTTT GCCATGATCA TCGTGGCTTC CTACACTGCC
GCATAGGATC CGTACCACAC CCGACCAAAA CGGTACTAGT AGCACCGAAG GATGTGACGG
T

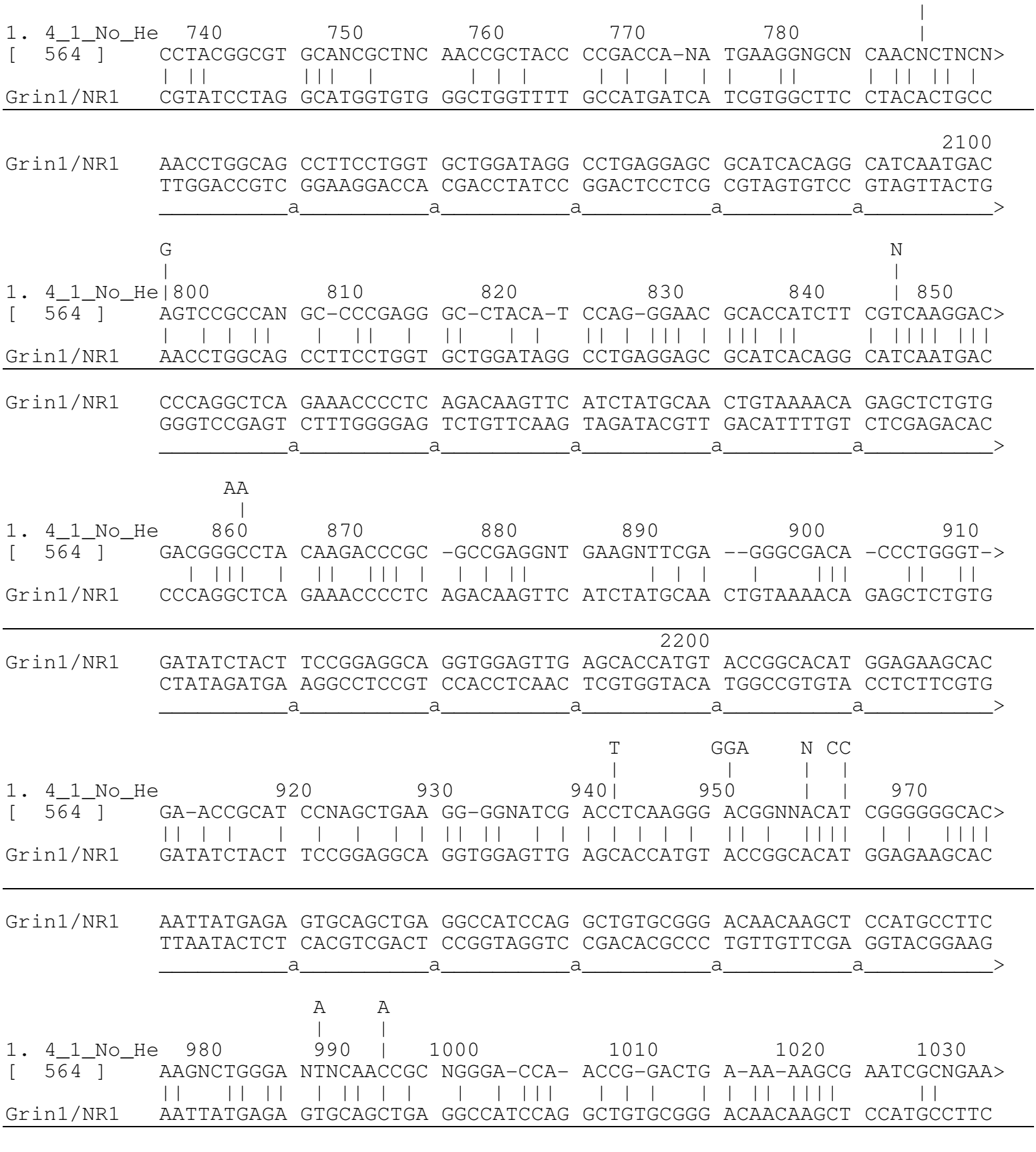
1. 4_1_No_He 740 750 760 770 780
[564] CCTACGGCGT GCANCGCTNC AACCGCTACC CCGACCA-NA TGAAGGNGCN CAACNCTNCN>
Grin1/NR1 CGTATCCTAG GCATGGTGTG GGCTGGTTTT GCCATGATCA TCGTGGCTTC CTACACTGCC
Grin1/NR1 AACCTGGCAG CCTTCCTGGT GCTGGATAGG CCTGAGGAGC GCATCACAGG CATCAATGAC
TTGGACCGTC GGAAGGACCA CGACCTATCC GGACTCCTCG CGTAGTGTCC GTAGTTACTG
1. 4_1_No_He 800 810 820 830 840 850
[564] AGTCCGCCAN GC-CCCGAGG GC-CTACA-T CCAG-GGAAC GCACCATCTT CGTCAAGGAC>
Grin1/NR1 AACCTGGCAG CCTTCCTGGT GCTGGATAGG CCTGAGGAGC GCATCACAGG CATCAATGAC
Grin1/NR1 CCCAGGCTCA GAAACCCCTC AGACAAGTTC ATCTATGCAA CTGTAAAACA GAGCTCTGTG
GGGTCCGAGT CTTTGGGGAG TCTGTTCAAG TAGATACGTT GACATTTTGT CTCGAGACAC
1. 4_1_No_He 860 870 880 890 900 910
[564] GACGGGCCTA CAAGACCCGC -GCCGAGGNT GAAGNTTCGA --GGGCGACA -CCCTGGGT->
Grin1/NR1 CCCAGGCTCA GAAACCCCTC AGACAAGTTC ATCTATGCAA CTGTAAAACA GAGCTCTGTG
Grin1/NR1 GATATCTACT TCCGGAGGCA GGTGGAGTTG AGCACCATGT ACCGGCACAT GGAGAAGCAC
CTATAGATGA AGGCCTCCGT CCACCTCAAC TCGTGGTACA TGGCCGTGTA CCTCTTCGTG
1. 4_1_No_He 920 930 940 950 970
[564] GA-ACCGCAT CCNAGCTGAA GG-GGNATCG ACCTCAAGGG ACGGNNACAT CGGGGGGCAC>
Grin1/NR1 GATATCTACT TCCGGAGGCA GGTGGAGTTG AGCACCATGT ACCGGCACAT GGAGAAGCAC
Grin1/NR1 AATTATGAGA GTGCAGCTGA GGCCATCCAG GCTGTGCGGG ACAACAAGCT CCATGCCTTC
TTAATACTCT CACGTCGACT CCGGTAGGTC CGACACGCCC TGTTGTTCGA GGTACGGAAG
1. 4_1_No_He 980 990 1000 1010 1020 1030
[564] AAGNCTGGGA NTNCAACCGC NGGGA-CCA- ACCG-GACTG A-AA-AAGCG AATCGCNGAA>
Grin1/NR1 AATTATGAGA GTGCAGCTGA GGCCATCCAG GCTGTGCGGG ACAACAAGCT CCATGCCTTC

```
                          2300
Grin1/NR1   ATCTGGGACT CAGCTGTGCT GGAGTTTGAG GCTTCACAGA AGTGCGATCT GGTGACCACG
            TAGACCCTGA GTCGACACGA CCTCAAACTC CGAAGTGTCT TCACGCTAGA CCACTGGTGC
            __________a__________a__________a__________a__________a__________>

               A
               |
1. 4_1_No_He   1040       1050       1060       1070          1080       1090
[  564 ]    ATTTAAGAGG CNTNTCNCCC CTANTTGGAC CAGGGACCG- -G-GGGANNG GGANAAAAAN>
            || |  ||   |   |   |    | || ||       || |   | | ||    ||  |  |
Grin1/NR1   ATCTGGGACT CAGCTGTGCT GGAGTTTGAG GCTTCACAGA AGTGCGATCT GGTGACCACG
```

```
                                                                        2400
Grin1/NR1   GGTGAGCTGT TCTTCCGCTC CGGCTTTGGC ATCGGCATGC GCAAGGACAG CCCCTGGAAG
            CCACTCGACA AGAAGGCGAG GCCGAAACCG TAGCCGTACG CGTTCCTGTC GGGGACCTTC
            __________a__________a__________a__________a__________a__________>

1. 4_1_No_He      1100       1110           1120       1130
[  564 ]    AACCANAGGN NCTTGGGGAN CGGNNANGG- --NGGTCTCC NNGGGGNCA>
                |   |   |||  |    |||    ||     ||  | |     || ||
Grin1/NR1   GGTGAGCTGT TCTTCCGCTC CGGCTTTGGC ATCGGCATGC GCAAGGACA
```

References

1. Anson, L.C.; Chen, P.E.; Wyllie, D.J.A.; Colquhoun, D. and Schoepfer, R. Identification of Amino Acid Residues of the NR2A Subunit That Control Glutamate Potency in Recombinant NR1/NR2A NMDA Receptors. *J. Neuros*ci. 18. (1998).

2. Baker PE, Kearney JA, Gong B, Merriam AP, Kuhn DE, Porter JD, Rafael-Fortney JA. Analysis of gene expression differences between utrophin/dystrophin-deficient vs mdx skeletal muscles reveals a specific upregulation of slow muscle genes in limb muscles. *Neurogenetics*. 7:2. (2006).

3. Bendová Z, Sumová A, Mikkelsen J.D. Circadian and developmental regulation of N-methyl-d-aspartate-receptor 1 mRNA splice variants and N-methyl-d-aspartate-receptor 3 subunit expression within the rat suprachiasmatic nucleus. *Neuroscience*.159:2. (2009).

4. Biben C, Hadchouel J, Tajbakhsh S, Buckingham M. Developmental and tissue-specific regulation of the murine cardiac actin gene in vivo depends on distinct skeletal and cardiac muscle-specific enhancer elements in addition to the proximal promoter. *Dev Biol*. 173:1. (1996).

5. Bradley J, Carter SR, Rao VR, Wang J, Finkbeiner S. Splice variants of the NR1 subunit differentially induce NMDA receptor-dependent gene expression. *J Neuroscience*. 26:4. (2006).

6. Bullock J, Boyle J, Wang MB. Physiology. 4 ed. New York: Lippincott Williams & Wilkins, 2001.

7. Campbell KP, Kahl SD. Association of dystrophin and an integral membrane glycoprotein. *Nature*. 338. (1989).

8. Campusano JM, Andrés ME, Magendzo K, Abarca J, Tapia-Arancibia L, Bustos G. Novel alternative splicing predicts a truncated isoform of the NMDA receptor subunit 1 (NR1) in embryonic rat brain. *Neurochem R*es. 30. (2005).

9. Choi DW. Glutamate neurotoxicity and diseases of the nervous system. *Neuron*. 1:8. (1988).

10. Colquhoun D, Jonas P, Sakmann B. Action of brief pulses of glutamate on AMPA/kainate receptors in patches from different neurones of rat hippocampal slices. *J Physiol (Lond).* 458. (1992).

11. Davies KE, Pearson PL, Harper PS, Murray JM, O'Brien T, Sarfarazi M, Williamson R. Linkage analysis of two cloned DNA sequences flanking the Duchenne muscular dystrophy locus on the short arm of the human X chromosome. *Nucleic Acids Res*. 11:8. (1983).

12. Dimario JX, Stockdale FE. Both Myoblast Lineage and Innervation Determine Fiber Type and Are Required for Expression of the Slow Myosin Heavy Chain 2 Gene. *Developmental Biology* 188. (1997).

13. Dingledine R, Borges K, Bowie D, Traynelis SF. The glutamate receptor ion channels. *Pharmacological Reviews*. 51. (1997).

14. Durand GM, Bennett MVL, Zukin RS. Splice variants of the N-methyl-D-apartate receptor NR1 identify domains involved in regulation by polyamines and protein kinase C. *Proc Natl Acad Sci USA*. 90. (1993)

15. Eagle M, Baudouin SV, Chandler C, Giddings DR, Bullock R, Bushby K. Survival in Duchenne muscular dystrophy: improvements in life expectancy since 1967 and the impact of home nocturnal ventilation. *Neuromuscul Disord*. 12. (2002).

16. Eagle M, Bourke J, Bullock R, Gibson M, Mehta J, Giddings D, Straub V, Bushby K. Managing Duchenne muscular dystrophy—the additive effect of spinal surgery and home nocturnal ventilation in improving survival. *Neuromuscul Disord*. 17. (2007).

17. Emanuel BS, Zackai EH, Tucker SH. Further evidence for Xp2l location of Duchenne muscular dystrophy (DMD) locus: X;9 translocation in a female with DMD. *J Med Genet* 20. (1983).

18. Forrest D, Yuzaki M, Soares HD, Ng L, Luk DC, Sheng M, Stewart CL, Morgan JL, Connor JA, Curran T. Targeted disruption of NMDA receptor 1 gene abolishes NMDA response and results in neonatal death. *Neuron* 13. (1994).

19. Francke U, Ochs HD, de Martinville B, Giacalone J, Lindgren V, Disteche C, Pagon RA, Hofker MH, van Ommen GJB, Pearson PL, Wedgwood RJ. Minor Xp21 chromosome deletion in a male associated with expression of duchenne muscular dystrophy, chronic granulomatous disease, retinitis pigmentosa, and McLeod syndrome. *Am J Hum Genet*. 37:2. (1985).

20. Feldmeyer D, Kask K, Brusa R, Kornau HC, Kolhekar R, Rozov A, Burnashev N, Hvalby O, Sprengel R, Seeburg PH. Neurological dysfunctions in mice expressing different levels of the Q/R site-unedited AMPAR subunit GluR-B. *Nature Neuroscience*. 2:1. (1999).

21. Gutmann E. Neurotrophic relations. *Annu Rev Physiol*. 38. (1976).

22. Hirai H, Kirsch J, Laube B, Betz H, Kuhse J. The glycine binding site of the N methyl-D-aspartate receptor subunit NR1: Identification of novel determinants of co-agonist potentiation in the extracellular M3-M4 loop region. *Proc. Natl. Acad. Sci., USA*. 93. (1997).

23. Hoess RH, Abremski K. Mechanism of strand cleavage and exchange in the Cre-lox site-specific recombination system. *J Mol Biol*. 181:3. (1985).

24. Hollmann M, Boulter J, Maron C, Beasley L, Sullivan J, Pecht G, Heinemann S. Zinc potentiates agonist-induced currents at certain splice variants of the NMDA receptor. *Neuron*. 10:5. (1993).

25. Hume RI, Dingledine R, Heinemann SF. Identification of a site in glutamate receptor subunits that controls calcium permeability. *Science*. 253. (1991).

26. Jacobs PA, Hunt PA, Mayer M, Bart RD. Duchenne muscular dystrophy (DMD) in a female with an X/autosomal translocation: further evidence that the DMD locus is at Xp2l. *Am J Hum Genet* 33. (1981).

27. Keinänen K, Wisden W, Sommer B, Werner P, Herb A, Verdoorn TA, Sakmann B, Seeburg PH. A family of AMPA-selective glutamate receptors. *Science*. 249:4968. (1990).

28. Kishimoto Y, Nakazawa K, Tonegawa S, Kirino Y, Kano M. Hippocampal CA3 NMDA receptors are crucial for adaptive timing of trace eyeblink conditioned response. *J Neurosci*.26:5. (2006).

29. Koenen M, Peter C, Villarroel A, Witzemann V, Sakmann B. Acetylcholine receptor channel subtype directs the innervation pattern of skeletal muscle. *EMBO reports*. 6:6. (2005).

30. Kohler M, Clarenbach CF, Bahler C, Brack T, Russi EW, Bloch KE. Disability and survival in Duchenne muscular dystrophy. *Journal of Neurology, Neurosurgery, and Psychiatry*. 80. (2009).

31. Köpke AKE, Bonk I, Sydow S, Menke H, Spiess J. Characterization of the NR1, NR2A, and NR2C receptor proteins. *Protein Science*. 2:12. (1993).

32. Koyuncuoğlu H, Kara I, Günel MA, Nurten A, Yamantürk P. N-methyl-D-aspartate antagonists, glutamate release inhibitors, 4-aminopyridine at neuromuscular transmission. *Pharmacol R*es. 37:6. (1998).

33. Küppenbender KD, Albers DS, Iadarola MJ, Landwehrmeyer GB, Standaert DG. Localization of alternatively spliced NMDAR1 glutamate receptor isoforms in rat striatal neurons. *J Comp Neurol*. 15:2. (1999).

34. Laube B, Hirai H, Sturgess M, Betz H, Kuhse J. Molecular determinants of agonist discrimination by NMDA receptor subunits: analysis of the glutamate binding site on the NR2B subunit. *Neuron.* 18. (1997).

35. Lee K, Park J, Kim K. NMDA receptor-mediated calcium influx plays an essential role in myoblast fusion. *FEBS Letters.* 578:1-2. (2004).

36. Mandel JL. Dystrophin: the gene and its product. *Nature*. 339. (1989).

37. Martin LJ, Blackstone CD, Levey AI, Huganir RL, Price DL. AMPA glutamate receptor subunits are differentially distributed in rat brain. *Neuroscience*. 53. (1993).

38. Mays TA, Sanford JL, Hanada T, Chishti AH, Rafael-Fortney JA. Glutamate receptors localize postsynaptically at neuromuscular junctions in mice. Mu*scle Nerve*. 39:3. (2009).

39. Merlie JP, Sanes JR. Concentration of acetylcholine receptor mRNA in synaptic regions of adult muscle fibres. *Nature*. 317:6032. (1985).

40. Miniou P, Tiziano D, Frugier T, Roblot N, Le Meur M, Melki J: Gene targeting restricted to mouse striated muscle lineage. *Nucleic Acids Res*. 27. (1999).

41. Moscoso LM, Merlie JP, Sanes JR. N-CAM, 43K-rapsyn, and S-laminin mRNAs are concentrated at synaptic sites in muscle fibers. *Mol Cell Neurosci*. 6:1. (1995).

42. Müller T, Möller T, Berger T, Schnitzer J and Kettenmann H. Calcium entry through kainate receptors and resulting potassium-channel blockade in Bergmann glial cells. *Science*. 256. (1992).

43. Muntoni F, Torelli S, Ferlini A. Dystrophin and mutations: one gene, several proteins, multiple phenotypes. *The Lancet Neurology*. 2:12. (2003).

44. Musshoff U, Schünke U, Köhling R, Speckmann EJ. Alternative splicing of the NMDAR1 glutamate receptor subunit in human temporal lobe epilepsy. *Mol Brain Res*. 76:2. (2000).

45. Nagy A. Cre recombinase: the universal reagent for genome tailoring. *Genesis.* 26. (2000).

46. Nakanishi N, Axel R, Shneider NA. Alternative splicing generates functionally distinct N-methyl-D-aspartate receptors. *Proc Natl Acad Sci USA*. 89. (1992).

47. Oh SJ. Clinical Electromyography: Nerve Conduction Studies. Lippincott Williams & Wilkins: 2002. pp. 10-12.

48. Ohlendieck K, Ervasti JM, Snook JB, Campbell KP. Dystrophin– glycoprotein complex is highly enriched in isolated skeletal muscle sarcolemma. *J Cell Bio.* 112. (1991).

49. Pizzi M, Brunelli G, Barlati S, Spano PF. Glutamatergic innervation of rat skeletal muscle by supraspinal neurons: a new paradigm in spinal cord injury repair. *Curr Opin Neurobiol*. 16:3. (2006).

50. Platt SR. The role of glutamate in central nervous system health and disease – A review. *Vet J.* 173. (2007).

51. Polo-Parada L, Plattner F, Bose C, Landmesser LT. NCAM 180 Acting via a Conserved C-Terminal Domain and MLCK Is Essential for Effective Transmission with Repetitive Stimulation. *Neuron*. 46. (2005).

52. Popik P, Layer RT, Skolnick P. The putative anti-addictive drug ibogaine is a competitive inhibitor of [3H]MK-801 binding to the NMDA receptor complex. *Psychopharmacology*. 114:4. (1994).

53. Prybylowski KL, Wolfe BB. Developmental differences in alternative splicing of the NR1 protein in rat cortex and cerebellum. *Developmental Brain Research*. 123:2. (2000).

54. Rafael JA, Townsend ER, Squire SE, Potter AC, Chamberlain JS, Davies KE. Dystrophin and utrophin influence fiber type composition and post-synaptic membrane structure. *Hum Mol Genet*. 9 (2000).

55. Rafuse VF, Polo-Parada L, Landmesser LT. Structural and Functional Alterations of Neuromuscular Junctions in NCAM-Deficient Mice. *J Neuroscience*. 20:17. (2000).

56. Rando TA. The dystrophin-glycoprotein complex, cellular signaling, and the regulation of cell survival in the muscular dystrophies. *Muscle Nerve*. 24. (2000).

57. Romberg C, Raffel J, Martin L, Sprengel R, Seeburg PH, Rawlins JN, Bannerman DM, Paulsen O. Induction and expression of GluA1 (GluR-A)-independent LTP in the hippocampus. *Eur J Neurosci*. 29:6. (2009).

58. Rothman DL, Hanstock CC, Petroff OA, Novotny EJ, Prichard JW, Shulman RG. Localized ^{1}H NMR spectra of glutamate in the human brain *Magn. Reson. Med*. 25. (1992).

59. Rumbaugh G, Prybylowski K, Wang JF, Vicini S. Exon 5 and spermine regulate deactivation of NMDA receptor subtypes. *J Neurophysiol* 83. (2000).

60. Sakakibara H, Engel AG, Lambert EH. Duchenne dystrophy: ultrastrutural localization of acetylcholine receptor and intracellular microelectorde studies of neuromuscular transmission. *Neurology*. 8. (1977).

61. Sakimura K, Kutsuwada T, Ito I, Manabe T, Takayama C, Kushiya E, Yagi T, Aizawa S, Inoue Y, Suglyama H, Mishina M. Reduced hippocampal LTP and spatial learning in mice lacking NMDA receptor ε1 subunit. *Nature*. 373:12. (1995).

62. Sakimura K, Bujo H, Kushiya E, Araki K, Yamazaki M, Yamazaki M, Meguro H, Warashina A, Numa S, Mishina M. Functional expression from cloned cDNAs of glutamate receptor species responsive to kainate and quisqualate. *FEBS Lett.* 272. (1990).

63. Sauer B, Henderson N. Cre-stimulated recombination at loxP-containing DNA sequences placed into the mammalian genome. *Nucleic Acids Res*. 17. (1989).

64. Sauer B, Henderson N. Site-specific DNA recombination in mammalian cells by the Cre recombinase of bacteriophage P1. *Proc. Natl. Acad. Sci. USA*. 85. (1988).

65. Schaeffer L, de Kerchove d'Exaerde A, Changeux JP. Targeting transcription to the neuromuscular synapse. *Neuron*. 31:1. (2001).

66. Single FN, Rozov A, Burnashev N, Zimmermann F, Hanley DF, Forrest D, Curran T, Jensen V, Hvalby O, Sprengel R, Seeburg PH. Dysfunctions in Mice by NMDA Receptor Point Mutations NR1(N598Q) and NR1(N598R). *J Neuroscience*. 20:7. (2000).

67. Stephenson FA. Structure and trafficking of NMDA and GABAA Receptors. *Biochem. Soc. Trans*. 34. (2006).

68. Sternberg N, Hamilton D. Bacteriophage P1 site-specific recombination. I. Recombination between loxP sites. *J Mol Biol*. 150:4. (1981).

69. Suen PC, Wu K, Levine ES, Mount HTJ, Xu JL, Lin SY, Black IB. Brain-derived neurotrophic factor rapidly enhances phosphorylation of the postsynaptic N-methyl-d aspartate receptor subunit. *PNAS*. 94:15. (1997).

70. Thoreux M, Olivant A, Akins RE. C Histomorphology of neuromuscular junction in Duchenne muscular dystrophy. *Pediatric Anesthesia*. 18. (2006).

71. Tsien JZ, Huerta PT, Tonegawa S. The essential role of hippocampal CA1 NMDA receptor-dependent synaptic plasticity in spatial memory. *Cell*. 87. (1996).

72. Verdoorn TA, Burnashev N, Monyer H, Seeburg PH, Sakmann B. Structural determinants of ion flow through recombinant glutamate receptor channels. *Science*. 252:5013. (1991).

73. Webster C, Silberstein L, Hays AP, Blau HM. Fast muscle fibers are preferentially affected in Duchenne muscular dystrophy. *Cell*. 52:4. (1988).

74. Weiss RG, Sterna MD, de Alubquerquea CP, Vandegaera K, Chackob VP, Gerstenblita G. Consequences of altered aspartate aminotransferase activity on ^{13}C-glutamate labelling by the tricarboxylic acid cycle in intact rat hearts. *Biochimica et Biophysica Acta*. 1243:3. (1995).

75. Worton RG, Duff C, Sylvester JE, Schmickel RD, Willard HF. Duchenne Muscular Dystrophy Involving Translocation of the dmd Gene Next to Ribosomal RNA Genes. *Science*. 224:4656. (1984).

76. Yuan H, Geballe MT, Hansen KB, Traynelis SF. Structure and Function of the NMDA Receptor. Structural And Functional Organization Of The Synapse. Edited by: Hell JW and Ehlers MD. New York: Springer. 2008. pp 289-316.

77. Zamanillo D, Sprengel R, Hvalby O, Jensen V, Burnashev N, Rozov A, Kaiser KMM, Koster HJ, Borchardt T, Worley P, Lubke J, Frotscher M, Kelly PH, Sommer B, Andersen P, Seeburg PH, Sakmann B. Importance of AMPA receptors for hippocampal synaptic plasticity but not for spatial learning. *Science*. 284:5421. (1999)

78. Zukin R, Bennet M. Alternatively spliced isoforms of the NMDAR1 receptor subunit. *Trends Neurosci*. 17:306. (1995).